# The implications of the lack of pulsar-orbiting planets on pre-supernova planetary orbital distributions

---

A Thesis
Presented to
The Division of Mathematics and Natural Sciences
Reed College

---

In Partial Fulfillment
of the Requirements for the Degree
Bachelor of Arts

---

Aaron Deich

May 2011

Approved for the Division
(Physics)

_____

Johnny Powell

# Acknowledgements

I'd like to thank Steve Thorsett for both suggesting this topic and giving his generous help in answering my questions throughout the year. It is entirely thanks to him that this particular thesis exists.

I'm grateful to Joel Franklin, David Griffiths, and Albyn Jones for their respective consultations on computation, writing style, and probability. I'd like to thank my thesis adviser, Johnny Powell, for his indispensable guidance, his unwavering heedfulness, and for generally being a hoot.

I'd like to thank my mother, father, and brother for being in all ways a heartening presence in my life. Particularly my brother, who helped me with some of the illustrations and editing. But particularly the other two as well.

# Preface

This thesis is written with two types of readers in mind: (1) for graduates of a freshman physics course who posses a decent level of scientific literacy, but for whom most of the basic astronomical concepts herein are novel, and (2), as a guide for future undergraduate students who might follow my path, or some portion of it – hopefully, this exposition and all of the referenced papers and books will offer help.

One of the nice aspects of non-relativistic astrophysics, compared with other areas of physics (such as ferromagnetism, quantum electrodynamics, or general relativity) is that it tends to appeal to our everyday intuition, spatially and dynamically. The background for the astrophysics of this thesis is provided for the sake of giving the reader a sense of physical backdrop, albeit sparse in details. My coverage of the thesis' theory (for instance, orbital mechanics, stellar evolution, etc) is trimmed of all but those parts which I consider necessary for consideration of my argument and conclusion.

# Table of Contents

# Abstract

In this thesis, a Monte Carlo simulation is performed to model the effect of a star's supernova explosion on its planetary system, with the goal of testing which planets are most likely to remain orbitally bound to the remaining neutron star core. The relevance of planets likely to survive is that, because there are no detected planets around pulsars which have survived supernova, such likely-survival planets are therefore less likely to exist around pulsar progenitors at the moment of the explosion. The simulation finds that the planets most likely to survive bear a .002 survival probability and are those with the semi-major axes of 2 AU (the smallest possible before engulfment by the giant pre-supernova star), while there is not clear dependence on orbital eccentricity. While this result allows a insight about the lower likelihood of the existence of planets in that orbital regime, the current number of detect pulsars (1,973) is too low to allow for strong non-existence predictions.

# Chapter 1

# A General Background

This chapter is a review of the astronomical bodies and processes relevant to this thesis. While not crucial to considering the calculations of Chapters 2 and 3, it is meant to provide the reader with a sense of the physical setting. Much of the work done in preparing this thesis was spent simply familiarizing myself with the metamorphoses of stars and planets, so that the calculation itself would make more sense. The following broad overview is meant not so much to firmly educate the reader as it is an introduction into the vast and fascinating environment of stars and planets.

## 1.1 An Introduction To Our Problem

As of April 2011, astronomers have detected a total of 531 planets outside of the solar system. All detected planets have occured only in two kinds of environment: (1), in the orbit of main-sequence stars and (2), in the orbit of pulsars (and given our current technology, there is no other environment whose planets *could* be detected). The *main-sequence* is the middle and longest period of every star's life; most of the stars you can see with the naked eye are on the main-sequence. A *pulsar* is the cold, dark, rapidly-rotating remnant left over after a massive star leaves its main-sequence, swells up, quickly collapses on itself, and explodes in supernova. Thus every pulsar was at one time a main-sequence star.

Now, a puzzling contrast: It is estimated that around 30% of stars, including those billions visible to us, posses planets [1]; thus the small number of discovered planets around stars reflects only a difficulty in detection. Yet of the 1927 known pulsars, only two have planetary systems ([2], [3]). This latter paucity is *not* due to detection difficulties (planets are much more detectable around pulsars [4]) but because truly all but two discovered pulsars are barren. The most basic question is, then, why are planets so much rarer around pulsars than around main-sequence stars? Do planets ever survive the tumultuous interlude between main-sequence and pulsar?

This thesis examines a model of the intervening stellar evolution and supernova explosion, and how it alters the orbit of a given planet. Which, if any, planets survive to the see the pulsar? If the model predicts a virtually zero survival-rate, perhaps we

have further evidence that planets can form from scratch around pulsars, from the debris left by the supernova.

## 1.2 A Timeline of Stellar Evolution

We survey the astronomical background to follow with a wide-view, yet simplified map of stellar evolutionary paths, shown in Fig. 1.1. Later in this chapter, we will examine each body or process in more detail. This panorama gives a rough overview of the setting of this thesis. Each point in the path is described below.

1. The starting point of the path is the stellar nursery, where large clouds of gas and dust gravitationally collapse on themselves to become protostars; if the material is rich enough in metals, protoplanetary disks will form too. Such star-yielding clouds of gas, incidentally, roughly match the initial stellar climate following the Big Bang, 13 billion years ago.

2. Next a given star enters the *main sequence*, during which it attains relative stability in temperature, size, and brightness for a long period of time. Its planetary system, if it has one, has stable orbits. The Sun, for instance, is currently in the middle of its 10-billion-year main sequence. This evolutionary stage is one of the only two on the timeline where we are capable of observing planets (the other is in the orbit of pulars).

3. When the star's primary fuel, hydrogen, runs low, the core switches to the hotter process of helium fusion. This hotter core causes the star's hydrogen shell to gradually expand and cool off. Here the star has become a *red giant*. It may swallow some of its innermost planets in the process of growth.

3.1 (exit option *a*). If the star's zero-age mass [1] is such that $m_0 \leq 8_\odot$ [2], its shell will blow away, revealing the dense, carbon-oxygen core, called a *white dwarf*. A white dwarf has stopped evolving. This will be the case with our Sun.

4. If the star's zero-age mass is such that $m_0 \geq 8_\odot$, the giant star will collapse on itself in a *supernova*, and on the rebound eject material in a spectacular explosion. What happens to the star's planets during the supernova is a primary question of this thesis. *Spoiler:* the planets are typically not "obliterated"; rather the question is whether they become gravitationally unbound (they usually do).

4.1 (exit option *b*). If the star's zero-age mass is such that $8_\odot \leq m_0 \leq 13_\odot$, a *neutron star* will emerge from the center of the supernova. If this neutron star spins fast enough, it gives off bright pulses which let us observe it, and we call it a *pulsar*. Pulsars are the only other body around which we can detect planets.

4.2 (exit option *c*). If the star's zero-age mass is such that $m_0 \geq \sim 13_\odot$, then the supernova will leave behind a body so massive that nothing, not even light, can escape, which is called a *black hole*. It is thought that on a long enough timescale, black holes can evaporate; for our purposes here, they are finished evolving.

*Repeat*: The debris blown off during the supernova, along with material blown off

[1] The *zero-age mass* is the mass of the star at the beginning of its life.

[2] The $\odot$ symbol refers to 1 solar mass $= 1.99 \times 10^{30}$ kg, a common unit for describing stellar mass.

during various parts of the star's life, as well as unused material from the original nursery, will all go on to repeat the sequence over again. This process tends to repeat itself, each iteration taking longer and longer, until the final heat death of the universe.

## 1.3 Exoplanets

### 1.3.1 Definition

Formally, an extra-solar planet, or *exoplanet*, is any body which orbits a star (which isn't the Sun) or star remnant, has enough mass that it forms a roughly spherical shape but not so much mass to permit nuclear fusion, and has cleared its orbital path of debris [5]. This recently updated definition (2003) came from the same governing body, the International Astronomical Union (IAU), which along similar lines of thought demoted Pluto to a dwarf planet in 2006 [5]. In this thesis, however, our casual definition of an exoplanet will be slightly broader: because we consider planets which, for various reasons, become orbitally unbound from their star and fly off into interstellar space, our definition will include such "rogue planets," even after they depart.

### 1.3.2 The recent triumphs of detection

For hundreds of years, astronomers have thought the existence of planets around other stars likely. The absence of detected extrasolar planets sat until recently on the waning list of features which make our home planet and solar system unique in the universe.

The detection of the first exoplanet in 1992 was one of the major scientific breakthroughs in astronomy in the last few decades. This first planet was discovered around the pulsar PSR 1257+12 [2]; the first planet around a main sequence star was discovered in 1995 [6]. Since then, the number of detected planets has skyrocketed to 531 as of April 2011 [7], and the detection rate itself continues to accelerate. The breakthrough which allowed this sudden flood of discovery was not one of theory, but of the development of more-sensitive equipment – spectrographs and imagers. Indeed, astronomers have well understood feasible planet detection methods since as early as the 1960's, as well as having formed extensive theories for planet formation. That's not to say that the planets detected aren't surprising: the results are discussed below.

Exoplanets are difficult to detect because they're so small, far away, and relatively dim. In fact, it is difficult even to completely resolve a main-sequence star itself; most appear, even to highly-sensitive telescopes, as single points of light. To give an idea of the angular size of a typical star to an Earth observer: if a star has a Solar radius and is 10 light years from Earth (this is not too distant by astronomical standards), an object of equivalent angular size is a jelly bean, observed 500 miles away. Thus those apparent points of light we see with the naked eye truly are points – only one or two rods in our eyeball might receive the light (or, in the case of an ideal telescope,

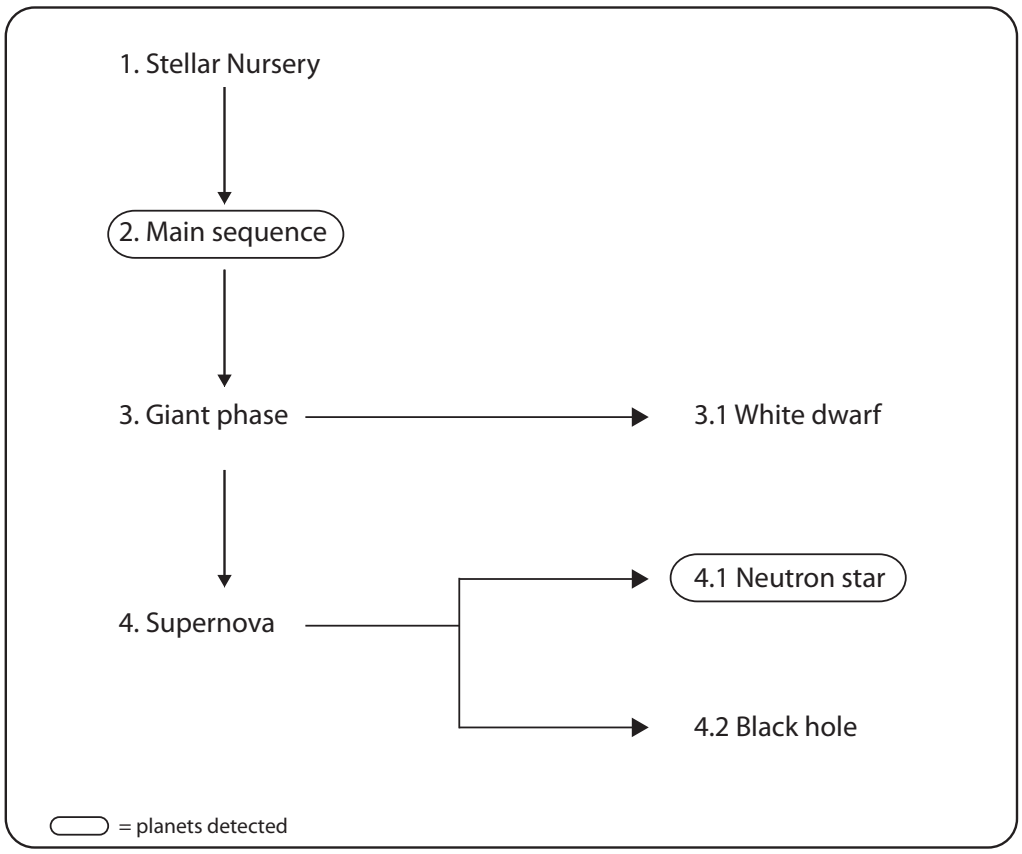


Figure 1.1: The timeline of a given star's life. The star's particular path through this map is determined by its initial mass: The smallest stars ($m_0 \geq 8_\odot$) will become white dwarfs, the mid-sized stars ($8_\odot \leq m_0 \leq 13_\odot$) will become neutron stars, and the largest stars ($m_0 \geq \sim 13_\odot$) will become black holes. Planets have only been detected around main-sequence stars and neutron stars.

light hits only one or two pixels out of an array of millions). Since stars are for the most part unresolvable, so are planets (for the most part)[3]; planets are typically less than 1/10th their star's size and much less luminous. Thus we can for the most part only detect exoplanets' presence via indirect means – studying their effect on their star's light output.

The two principle means of doing so are (1) the *radial velocity method* and (2) the *transit method*. The first measures the spectrum of light over time given off by the planet's star. Because the orbital system rotates around its common center of mass, the planet induces a wobble in the star. If this wobble is in a direction roughly towards the Earth, the light the Earth receives is Doppler shifted (higher frequency as the star approaches us and lower as the star recedes), and the spectrum of its light will oscillate up and down in time with the planet's orbit. The second detection method, that of transit, detects those planetary systems where the planet's orbit passes in between the Earth and the star. When the planet blocks some of its star's light, we observe the star's brightness periodically diminish.

A difficulty with these methods is that the signal-to-noise ratio is very small (the relatively miniscule planet induces a relatively miniscule effect on the star's light) so to pick out the planet-revealing periodicity in the starlight requires a lot of observation time (typically on the order of months to years). Thus these detection methods have a strong bias towards bigger planets (which cause the star to wobble more, or which block more light) and planets close in to the star (observation of their shorter orbital periods requires less timing data). Further, the detection methods fail for stars of great size or mass, whose light outputs are less affected by their planets. Currently, the largest star with a detected planet has a mass of $2.10_{\odot}$ [7].

The thesis of Ryan Lau (Reed '10) includes a fantastic review of current exoplanets, well aimed at an undergraduate audience.

### 1.3.3 Where can exoplanets exist?

As discussed in the previous section, there are two environments where astronomers have actually detected exoplanets: around main-sequence solar-type stars, and around pulsars.

It is estimated that roughly 30% of main-sequence stars have planetary systems [1]; that astronomers can see tens of millions of main-sequence stars but only 531 exoplanets is due to a difficulty in detection. A group has even found a binary star system which bears a planetary companion [9], though this is thought to be an extraordinary occurence.

Pulsars tend to be, on the other hand, barren of planets; of the known ∼1900 pulsars, only two bear planetary systems. This dearth of detection reflects a true lack of existence, not detection difficulty [4]. Planets around pulsars pose interesting questions, a few of which are the focus of this thesis. Namely, how did the planets get there? As mentioned in the Timeline of Stellar Evolution (Section 1.2), pulsars

[3]Several planets have been directly imaged, thanks to both extraordinary circumstances and improving search methods. In 2008 in particular, a team using the Hubble telescope resolved a planet around the star Fomalhaut [8].

are the cold, rapidly spinning remnants of main-sequence stars. A big question is whether planets can survive the star's violent metamorphosis into a pulsar, or if the planets around pulsars more often form from material after the pulsar's formation. Pulsars will be discussed in more detail in Section 1.5.2 below.

Planets can potentially exist in orbit around white dwarfs and black holes. While orbits around white dwarfs are possible, the likelihood is much lower than that around main-sequence stars. Several calculations have shown that planetary systems around white dwarfs are highly unstable and don't last very long [10]. None have been detected to date, either, though there are candidates [11]. Likewise, planets are certainly able to orbit black holes, though they are virtually impossible for us to ever detect.

Lastly, for every planet in a bound orbit, there is probably at least one other planet orbiting nothing – flying through interstellar space [1]. Most such planets were born in protoplanetary disks around young stars and were slingshot from their original stellar orbits by other young planets, during the high orbital instability characteristic of young planetary systems. As a note, these rogue planets are actually considered *ex*-planets by the technical definition cited in Section 1.3.1. To an observer on a recently ejected planet, however, the planet's appearance would change little, except that surface temperatures would quickly drop to those of interstellar space [12].

### 1.3.4 Planets' birth and orbital evolution

The theory of planet formation is one of the least mature of those described in this chapter and thus it is difficult to discuss without also covering the long list of the theory's observational and physical constraints. In comparison, introducing a more mature theory, such as that of stellar birth, does not generally require arguments for the theory's justification. At the scope and level of this thesis, it is sufficient to give only a rough sketch of planet formation and then describe (1) the theory's prediction of planetary distributions which are probable around stars, and (2) the conditions in which planets may form at all. For a good recent review of planet formation theory, see Mordasini et al, (2010) [1]. An excellent list of technical and general publications is included in Carroll and Ostlie (2007) [13].
The process of planet birth is generally simplified into discrete stages which are assumed to occur sequentially:

1. Accretion disks form with young stars, due to the angular momentum inherent in the system. The micrometer-sized dust particles of the disk stick together due to the electrostatic force. Once a given clump of dust grow large enough, the gravitational force dominates and planetesimals are formed. Planetesimals grow to about 100 km.

2. Planetesimals grow into protoplanets of roughly 1000 km in size. Some of the bodies can grow so large that they can accrete large gaseous envelopes.

3. The last stage is initiated when thermonuclear ignition begins in the young star, and the ensuing stellar wind drives away all gas and dust which hasn't accreted

onto protoplanets. The remaining planetary system tends to stabilize.

The primary important result of planet formation theory for this thesis is that it predicts that more massive stars have greater numbers of planets. And since we are considering the mighty pulsar progenitor stars, but can only see planets which orbit small, solar-type main sequence stars, the prediction gives us confidence in the former's sizable planetary population.

## 1.4 Stellar Evolution

The following exposition of stellar evolution is greatly condensed, perhaps by a factor of 20 from the detail level of an undergraduate text. This is because (1) stellar evolution is such a complex and episodic story that to describe any single part in detail would warrant equal treatment of the whole, which would be too long; (2) because our primary concern, that of the narratives of planets, ultimately cares only about the star's external effects, e.g. its gravitational pull; whether its radius engulfs the planet; the tidal forces on the planet; etc. and (3) because the intricacies of stellar evolution are ultimately of lesser importance to this thesis' question of planet survival, given the way the argument is framed.

### 1.4.1 Star birth

The material which will go on to compose a given star resides initially in a cloud of interstellar medium. The interstellar medium (ISM) permeates galaxies in a continuous and fluctuating spread, and when we say "clouds," we mean areas where the ISM is much more dense. A cloud which will lead to a star is, at the outset, big, cold, and ever-so-slightly denser than vacuum. The cloud expands or contracts primarily depending on the difference between two opposing forces within it: gravity, which exerts a collapsing force; and gas pressure, which exerts an expanding force.

Such clouds have a size on the order of 10 parsecs, roughly $10^4$ times the size of our solar system. Clouds float dormant in hydrostatic equilibrium, and will not begin to shrink, until they either (a) lose pressure due to cooling, (b) accrue enough mass by colliding with other clouds or (c) experience a shock wave from somewhere else (possibly a supernova); at which point gravitational collapse begins.

If the cloud is bigger than a certain size, it will not shrink towards a single center, but will instead collapse around multiple points, thus separating into smaller clouds. This division process will repeat in a fractal-like fashion until a given fragment reaches a roughly stellar mass and will collapse entirely around a single point.

The cloud is composed typically of around 70% hydrogen with most of the remainder helium. Any heavier elements present were created earlier, either in stars or in supernovae, since the big bang produced almost entirely hydrogen and helium; the heavier elements may play a role in determining the size of the protostar.

While a number of more nuanced processes occur as the rotating sphere of gas shrinks, the net result is a protostar, which is sufficiently hot and dense for the hydrogen to begin fusion.

By the time a protostar has formed, its ultimate fate is sealed, because a star's so-called zero-age mass entirely determines its following evolution.

A brief description of why fusion occurs in stars: As a simplest explanation, the molecules of a gas have an average speed which increases with the gas's temperature; the molecules' constant bouncing into and off of each other give the gas its outward pressure. The actual physical "bounce" between two molecules is due to the Coulomb potential energy barrier between their two positively-charged nuclei, which are driven apart before they can get too close (the Coulomb potential goes as $1/r$). However, if the temperature grows high enough, molecules are given enough speed that nuclei can draw sufficiently close that their attractive, highly short-range nuclear force overpowers the Coulomb force and fuses the two nuclei together. In this fusing process, an enormous amount of energy is released. This simplest explanation is basically right, but it omits a few crucial mechanisms, such as quantum tunneling, which collectively reduce the required temperature for fusion by several orders of magnitude, down to agreement with the temperatures observed in stars.

As a sidenote, we tend to associate nuclear fusion with incomprehensible explosive power, due to its weaponization or the notorious difficulty in building an electricity-generating fusion reactor. The hydrogen fusion which tends to occur in stars, however, is actually much tamer. The average energy released per unit volume in the core of a main-sequence star is on the order of that of the human body [13]. Yet star interiors are much hotter ($10^3$K – $10^5$K) than humans because of the former's great heat-generating volume and insulating properties.

### 1.4.2 The main sequence

Once the protostar's nuclear fusion has begun, the star goes through a brief tumultuous period before settling down into relative stability, entering the *main sequence*. Because of the predominance of hydrogen in the star's initial composition, and since hydrogen fusion is a relatively slow process, the main sequence is by far the longest stage of a star's life. For this reason, about 90% of the stars we see with the naked eye are on their main sequence.

The physical characteristics, such as size, composition, output spectrum, and time span of the main sequence are, as mentioned above, entirely predetermined by the initial mass and composition of the protostar. The greater the star's initial mass, the shorter its main sequence. This is because, speaking in qualitative terms, the greater a star's mass, the hotter it will be, and the faster it will convert hydrogen into helium. The largest stars (mass on the order of $500_\odot$) have main-sequence life spans on the order of $10^5$ years, while the smallest stars (mass of around $0.1_\odot$) have lifetimes of order $10^{10}$ years, some longer than the current age of the universe. Our own Sun is, at this moment, in the middle of its roughly 10 billion year main sequence.

An efficient negative feedback mechanism is responsible for the main sequence's stability. As the star converts hydrogen into helium, the average molecular weight of the material in its core increases, causing the pressure to drop. With insufficient pressure in the core to support the overlying layers of the star, the star will shrink,

converting gravitational potential energy into heat, thus heating up the core and returning to the initial conditions. Over the long term, this process's net effects include a slow increase in the star's luminosity, radius, and temperature. [13, page 450].

The main sequence ends when the mass of the core becomes so great that the core can no longer support the weight of the star's upper layers.

### 1.4.3 Late life and death

The star's main sequence ends when the star begins to run out of hydrogen in its core; without the outward pressure generated by the hydrogen fusion, the core contracts, becoming hotter in the process. As a note, the star is not homogenous in its composition by this point – because the core is the only region in the star with high enough temperatures and pressures to cause fusion, the outer shell of gas remains largely unchanged from the original hydrogen-dominated composition of the protostar. As the core heats up following the exhaustion of the core's hydrogen, the star's low-density gaseous shell expands and cools. The star is now some kind of *giant*.

Helium is the main product of hydrogen fusion, and thus the core is helium rich by the time its hydrogen runs low. This higher density of helium serves to additionally contract and heat the core along with the hydrogen deprivation. The resulting hot temperatures eventually lead to ignition of helium fusion in the core, which requires much higher temperatures than hydrogen fusion.

The stellar envelope's enormous expansion is of great consequence to planets orbiting their star at small radii. The Sun, for instance, will swell to over 1 AU, thereby consuming all the inner planets. While the radii achieved by the massive pulsar progenitor stars ($\sim 10_{\odot}$) are not precisely known, they are estimated to approach 2 or 3 AU.

The final form of a star is determined by its initial mass by roughly

| Initial Mass | $m_0 \leq 8_{\odot}$ | $8_{\odot} < m_0 \leq 13_{\odot}$ | $13_{\odot} < m_0$ |
|---|---|---|---|
| End Result | White Dwarf | Neutron Star | Black Hole |

### 1.4.4 Supernovae

A *supernova* is the violent collapse and ensuing expulsion of debris which ends the life of all large stars (those with zero-age mass greater than $\sim 8_{\odot}$). Supernovae can radiate so brightly that during the few hours of highest intensity, they outshine their galaxies. While an orbiting planet might observe the supernova to be a simple, ferocious explosion, the timeline of a supernova is surprisingly and exhaustingly complex. We go into slightly deeper detail here than on other aspects of stellar evolution because supernovae play a central role in this thesis. The details will not end up mattering much for our simple classical model in Chapter 2, but we think it's important to observe the complexity of the processes going on 'under the shell.' The following subject matter is included in most astrophysics textbooks. We particularly recommend Carroll and Ostlie, 2007 [14] and Tassoul and Tassoul, 2004 [13].

Towards the end of the main sequence, helium burning begins a conversion to a stellar core of carbon and oxygen. These elements are normally quite resistant to fusion, but the pressures created by a massive star are sufficiently extreme for ignition. This evolutionary point is where a less massive star, its core left inert, would blow away its hydrogen-dominated shell, leaving behind the carbon-oxygen core – a new white dwarf.

But as stated above, massive stars heat their carbon and oxygen to the point of fusion. A variety of byproducts of this oxygen-carbon burning creates a new core dominated by $^{28}_{14}$Si; the core temperature continues to rise with the core's density; at $3 \times 10^9$ K, silicon burning can commence through a series of different reactions, many of which produce nuclei near the $^{56}_{26}$Fe energy peak. (Iron has the greatest binding energy of any element; thus fusion [an exothermic process] always morphs lighter elements in iron's direction, as fission does likewise to heavier elements). The time scale of each successive reaction is shorter than that of its predecessor because the energy released becomes smaller and smaller with approach of the iron peak. The result is an accelerating chain of reactions, the last of which take around an hour.

The dying star, by this point, has an interior layered like an onion, and with an iron core. Subsequently, photodisintegration strips iron down to individual protons and neutrons. An endothermic process, photodisintegration cools the core, removing the pressure necessary to support the rest of the star. Further lowering the core's pressure, the free electrons which have hitherto assisted in supporting the star through degeneracy pressure are captured by the free protons released by photodisintegration.

The total effect is that the core, suddenly a body of waning pressure but still of extreme mass, gravitationally collapses on itself. Near the core's center, the collapse is homologous, which is to say that a given atom will travel towards the center while remaining close to its original neighbors. This inward acceleration of a given chunk of the homologously-collapsing region is proportional to its distance from the center. However, there comes a certain radius where the inward acceleration demands too much of its medium, and the medium tears apart (this is where the inward velocity exceeds the local speed of sound). At this radius of tearing, the inner core is said to decouple from the now supersonic outer core, which is left suspended above a vacuum and nearly in free-fall. During the collapse, the outer core can reach inward speeds of $7 \times 10^4$ km s$^{-1}$ (which is roughly $0.2c$).

The homologous collapse of the innermost core meanwhile continues until the moment its density reaches about $8 \times 10^{17}$ kg m$^{-3}$, roughly three times that of an atomic nucleus. This maximum density barrier is that of neutron degeneracy pressure, a consequence of the Pauli exclusion principle applied to neutrons (see Section 1.5.1 for further explanation). The inner core is now a freshly-made neutron star, sitting at the center of the inward-falling shell. Immediately at its sudden halt of collapse, the inner core rebounds somewhat, sending pressure waves outward through itself. As this wave reaches the sound speed, another shock wave is produced, like that described above, only moving outwards.

Finally, the two massive shock waves collide, producing enormous temperatures. Perhaps counterintuitively, the high temperatures cause photodisintegration, which in turn robs the total shock of much of its energy. If, however, the neutrinosphere

heats this stalled shock quickly enough, the shock drives all of the nuclear-processed material away from the star. As an interesting note, this period of endothermic photodisintegration is responsible for producing much of the heavier elements (e.g., uranium) found on Earth.

The end result is that all material outside of the core is blown away at relativistic speeds (again, around $0.2\,c$). This material spreads out into a large cloud or nebula, similar to that which formed the initial protostar. The remaining core is either a neutron star or black hole, depending on whether the mass is less than or greater than $\sim 2.5_{\odot}$[4] Although "remaining" is not quite an accurate description, spatially speaking: supernovae have been recently determined to exert their explosive force asymmetrically, causing the core to experience a large net force in some direction. The core thus receives a *kick velocity*, shooting away from the explosion point. Empirical measurements of the galactic speeds of pulsars (those neutron stars visible to us) show that kick velocities are well described by a Maxwell-Boltzmann distribution with a mean of about 300 km $s^{-1}$ [17] (see Fig. 2.5). This speed is high for so massive a body. For comparison, the Earth's orbital speed around the Sun averages about 30 km $s^{-1}$, and the Sun's orbital speed around the galactic center is about 220 km $s^{-1}$. Some neutron stars are even thought to possess galactic escape velocities.

### 1.4.5 Stellar evolution's effect on planetary orbits

Having discussed both planetary formation and stellar evolution, we now examine the changes wrought by the star on its planet's orbit, from planet birth to the time of supernova. To reiterate our grand intent, we are ultimately curious about those specific planets which we predict *ought* to survive supernova and thence orbit pulsars. This section is motivated by a desire to identify such planets at their supernova moment with their younger counterparts, which in turn are detectable around main-sequence stars. That is, if given the orbit of such a future pulsar-planet at the moment before supernova, could we work backwards and determine how its orbit might have looked when the star was young? If such a computation were possible, we'd be able to compare the theoretically-predicted young planets to those exoplanets actually detected. Exoplanets, as a reminder, are only detectable at the present around small main-sequence stars, not around giants.

Sadly, a simulation of the evolution of a planet's orbit turns out to be far beyond the scope of this thesis and, often, in general. Most individual effects on orbit, described below, are basically understood; their net sum makes for an extremely complex numerical simulation, especially given the duration of a single star's evolution. For a good example of a simulation see [Villaver and Livio (2007)] [18].

Thus we relegate this thesis' most ambitious goal to the study of possible orbital

[4]The neutron star mass has long been considered to reside consistently around the canonical value of $1.4_{\odot}$, according to both theory and the measurements of binary systems containing neutron stars. However, a few recent papers ([15], [16]) find that the mass can range up to $2.5_{\odot}$ before collapsing into a black hole. While this increased mass is of great consequence for the computation of an individual planet's survival, the average mass is consistent enough that the following chapters assume simply a constant $1.4_{\odot}$ value.

distributions of planets *only* at that moment before supernova; all prior orbital history will remain unexplored.

For the sake of illustrating the complexities of orbital evolution and for giving a rough idea of why we choose to avoid the problem altogether, we next describe a few of the many effects which cause planetary orbits to change.

To a first order approximation and on the timescale of a few orbital periods, a given planet's orbit is well described by the Newtonian two-body problem (see Chapter 2), where two point-masses interact in a closed system only via the gravitational force. In such a model, orbital frequency and path remain constant in time. The short term accuracy of the approximation allows, for instance, an astrophysics textbook to list the various orbital parameters of the Solar System's planets without needing to be frequently reprinted – the parameters are stable enough that they won't change significantly over the next 1000 years.

However, planets do, at one extreme, spiral into their star; at the other, they become gravitationally unbound, leaving their star forever. In any case, if at least one of the bodies in a given two-body orbit is transforming in some way, the orbit itself is in flux[5]. The two failings of the simple two-body model above are that (1) in actuality the star's mass is always decreasing (though at a highly-varying rate), which serves to increase the orbit's size and slow the period; (2), there are a large number of complicating effects. Important effects are listed below.

- *Stellar mass loss*: Unless there is infalling matter, stars are continually losing mass, both during the main sequence and giant phase. The mass loss usually takes the form of stellar wind, where mostly protons and electrons are ejected from the star. For small stars, the mass loss during the main sequence is fairly well understood. The Sun, for instance, will have lost about 30% of its current mass by the time it begins its red giant phase in 5 billion years (the Earth will subsequently have drifted to a much larger orbit)[12]. Though such a mass loss is indeed a radical change for the Sun, that it occurs over such a large time span justifies our calling the main sequence 'stable.' Large stars' mass loss, on the other hand, is not well understood, particularly during their giant phase. Some estimates show that stars with zero-age mass greater than $8_{\odot}$ can lose as much as half of their original mass by the time they undergo supernova [13, 476].

  Stellar mass loss tends to exert no net force on the star, since we assume it occurs symmetrically. Thus the orbital system maintains a constant angular momentum per unit mass. Assuming that the mass loss occurs on a time scale much greater than a planet's orbital period about the star, the orbital radius will slowly increase. If the star loses enough mass, the system can become unbound altogether. It is certainly possible to model the comprehensive orbital evolution, from start to finish, if we are given the star's mass as a function of

[5]For instance, a two-planet system where both are tidally-locked will have reached a permanent orbit, neglecting the minute energy dissipations described by General Relativity.

time for the whole life of the star. But because such functions are so poorly understood, modeling of the orbital evolution ends up with prohibitively high uncertainty for massive stars.

- *Tidal forces*: Since a body in orbit (say, the Sun) is not rigid, and because the gravity acting upon it (by, say, the Earth) is stronger on the near side than the far side, the one body has a tendency to stretch out along the line towards the other. This distorting force is called the *tidal force.* As to how it affects orbit: if one of the bodies is rotating about its axis at a different rate than the system's orbital period (assuming the orbit is fairly circular), the body's elongation will have to continuously adjust to the changing relative position of its orbital companion. This results not only in a torque on the body, slowing its rotation speed, but also a widening and slowing of the orbit. For a good basic explanation of the tidal force, see [13].

- *Gas drag*: If a planet gets too close to its star's surface (though often "surface" is really a gradual transition from vacuum to gaseous shell) the planet will experience *gas drag.* When the gas moves slower than the planet, the planet decelerates. This theft of kinetic energy causes the planet's orbit to shrink. Most often, the affected planet ultimately enters a mortal spiral, heading into the depths of the star [18]. When we say that a gradually expanding giant star consumes its inner planets, those planets aren't truly "eaten" until gas drag quickly captures them above the star's surface. Simulating the effects of gas drag require knowing the gas's density and speed as a function of stellar radius and time.

- *Other planets' gravitation*: Most planetary systems are thought to contain multiple planets; in this case the Newtonian two-body description is still roughly sufficient for each individual planet – most of the system's mass is contained in the star. However, as the planets are also gravitationally attracted to one another, over a long time period large orbital perturbations can occur. Often a planet is ejected from the system. This is particularly true of young planetary systems. Simulation of orbital perturbations can either be complex numerical n-body simulations or simple probability distributions of likely outcomes.

- *Stellar wind*: Besides carrying away mass from the star, stellar winds can also alter the mass of planets. In the case of close-in gas planets, so called "hot jupiters," stellar winds are thought to strip gas from the planets' surface, lowering the planets' mass and increasing the size of orbit. Other planets can gain mass from stellar winds through retention of the particles, though the orbital effects of this process are probably negligible [19].

For a great example of such a simulation, see [Schroder and Smith (2008)] [12], which models the outcome of the Earth in the Solar System's future evolution (the Earth will most likely be engulfed by the Sun).

## 1.5 Neutron Stars (Particularly, Pulsars)

As a reminder, the importance of neutron stars in this thesis is that they are the only other object besides main-sequence stars around which planets have been detected.

### 1.5.1 Physical description

Neutron stars are the highly dense, collapsed cores of giant stars, compressed by gravity and supported by neutron degeneracy pressure. With a diameter of about 20 kilometers and an enormous mass of $\sim 1.4_{\odot}$, their density of $6.65 \times 10^{17}\,\mathrm{kg\ m^{-3}}$ is roughly three times that of the typical atomic nucleus [20]. At this density the entire human race would fit into a one-inch cube. The acceleration of a test mass due to gravity at the surface of a neutron star is equally extreme – about $10^9$ times that of Earth.

Degeneracy pressure, that effect responsible for supporting the neutron star and preventing it from contracting any further, is a result of the Pauli exclusion principle. Multiple quantum particles cannot occupy the same state and position, so they reach a point where in order to be within a certain range of each other, they must occupy different energy states.

Neutron stars have thin crust of normal atomic nuclei, mostly iron, crushed by the immense gravity into a lattice. As one proceeds deeper into the neutron star, the nuclei become increasingly filled with neutrons. The nuclei become smaller and smaller until the composition is almost entirely composed of a superconducting Fermi liquid of neutrons, protons, and electrons in a ratio of 8:1:1, in that order. In this sense, atoms tend to lose their identity, being broken up into their constituent parts.

Neutron stars usually have enormous magnetic fields, of order $10^{12}$ gauss. For comparison, the average magnetic field strength on the surface of the Earth is about 0.5 gauss. Neutron stars' magnetic fields are thought to have been conserved in total magnetic vector potential from their progenitor star; the condensation of the star during supernova equally condensed the magnetic field, resulting in its incredible strength.

### 1.5.2 Pulsars: rotating neutron stars

Since most neutron stars quickly cool after the supernova, they emit negligible blackbody radiation. Astronomers observe, instead, those neutron stars which are rapidly rotating: in sweeping their powerful magnetic fields around, they emit a lighthouse-like beam of electromagnetic radiation. Such rotating neutron stars are called *pulsars*, due to the pulse-like nature of their signal; they are, for the most part, the only neutron stars directly visible to us.

Pulsar rotation periods range from 5 seconds to 1.4 milliseconds; for a 20 km body with a mass greater than that of our Sun, these are incredible rotation speeds by Earthly standards. The centripetal acceleration alone at the surface of the pulsar ranges between $\sim 10^5$ and $\sim 10^9$ times that of a body falling due to the gravity on the Earth's surface.

The emission mechanism of pulsars is not well understood, but the basic model is that the pulsar's magnetic axis is offset from its rotation axis – thus for a given point in space outside the pulsar, the magnetic field is constantly changing in time; regions of this rotating magnetic field induce an electric field which produces and accelerates charged particles. Pulsar emissions occur primarily in two regimes: low-energy (radio) and high-energy (optical, X-ray, and gamma-ray). Modeling the emission mechanism is today a large and difficult open problem in pulsar astronomy, and the primary models' complexities are intimidating.

A given pulsar, if left alone, is always slowing down. Its rotating magnetic field acts as a brake, converting the pulsar's mechanical energy into electromagnetic emission. This angular deceleration is a function of the rotation speed and size of the magnetic field; thus the brightest pulsars slow down the fastest. It is estimated that the typical pulsar begins its life with a period less than 100 milliseconds (the initial source of this rotation is mostly due to a conservation of angular momentum of the progenitor star, since the neutron star has such a smaller angular inertia). Most pulsars will slow down to the point that their radiation is no longer visible on a timescale of $10^6$ to $10^8$ years. This estimate is consistent with a galactic birthrate of 1 pulsar every 50 years, which agrees with the estimated frequency of supernova events in our galaxy.

However, pulsars are not always slowing down because they're not always left alone. There exist high-speed *millisecond pulsars*, so called because of their order-of-milliseconds periods, which have been rotationally accelerated by infalling matter from an orbital companion, usually a white dwarf.

### A Brief History of the Observation of Pulsars

Pulsars were discovered unexpectedly in 1967 by graduate student Jocelyn Bell and her adviser at the Jodrell Bank Observatory. Bell had just begun surveying a certain region of the sky with a new radio telescope when she noticed a train of mysteriously regular pulses. Once it became clear the odd signal did not come from a terrestrial source, Bell and her adviser, Antony Hewish, insightfully suggested the signal was probably that of a rotating neutron star [21], a body which had remained until then only a theoretical concept. Neutron stars had first been proposed in 1934 by Walter Baade and Franz Zwicky [22], who had concluded them the likely end result of certain stellar evolution models. In the intervening 33 years, various theoretical physicists advanced predictions of the density, composition, and magnetic field of the theoretical neutron stars. Just before the 1967 discovery, Pacini [23] proposed that the rapid rotation of a highly magnetized neutron star might be the source of energy in the Crab Nebula (this has since been confirmed – the 'Crab Pulsar', PSR B0531+21, with its bright beam of charged particles makes the surrounding nebula glow).

The first pulsars detected, starting with Bell's discovery, were radio pulsars with slower rotation periods (on the order of 1 second) and with very pronounced signals; they were thus readily apparent to observers. But in the ensuing decades, further pulsar surveys, which consist of scanning various regions of the sky and looking for the telltale periodic signal, searched for increasingly muted and high-frequency oscillations. Most pulsar searches today hunt for millisecond pulsars, which tend to

emit in the x-ray and gamma ray spectrum. Such discoveries require many months to years of timing data in order to reveal any periodicity in a signal which appears otherwise random noise. To date, there have been 1,973 confirmed pulsars discovered ([24], [25]) and this number is expected to increase.

### 1.5.3 Planets around pulsars

In 1992, the first extra-solar planet ever was discovered around pulsar 1257+12 by A. Wolszcan [2]. The planet, actually part of a multi-planet system, was detected through a sort of radial velocity method: the period of the pulsar's signal had an oscillatory behavior of its own, due to the pulsar's wobble induced by the planetary system. There is a rich and thorough examination of the subfield, *Planets Around Pulsars* (ed. J. A. Phillips, S. E. Thorsett, and S. R. Kulkarni (1993)) [26], which is an important grounding for this thesis.

It turns out that pulsars, unlike main-sequence stars, yield a very precise measurement of whether they possess planets, due to the extreme regularity of their pulse signals [4]. Further, all but 2 of the $\sim 1900$ known pulsars are devoid of planets. To be precise, they are devoid of planets within a given regime of detectability – planet masses greater than $10^{-3}$ Earth masses and orbital periods less than a few years [4].

Sadly, the two detected pulsar planetary systems, one around PSR 1257+12 and the other around PSR 1620-26, do not represent the supernova survival events we specifically study in this thesis. For the the former's planets are so close in and their orbits all so consistently circular that the planets are thought to probably have coalesced from debris from the supernova explosion [26] rather than formed with the pulsar progenitor star; the latter, PSR 1620-26, is actually in a binary system with a white-dwarf companion, and so is governed by different, more complex models than we consider in Chapter 2. To summarize, no planets have been detected around pulsars which have survived supernova. These are the planets which we study in the following chapters.

And so we reach a central question of this thesis: what does this absence of planets around pulsars imply about the planets around pulsar progenitors, those giants on the verge of collapse? In considering this question, we model the effect of a supernova explosion on an orbital system, and with that model, we ask if it is possible that a planet could survive at all.

# Chapter 2

# Modeling the Effect of a Supernova On a Two-Body System

## 2.1 Orbital Mechanics

In this chapter we make precise and develop the model of what happens to a planet when its star explodes in supernova. To that end, we first consider the foundational problem of the dynamics of two bodies in space, if we know their starting conditions. That is, given an isolated system consisting of two spherical bodies[1] with masses $m_1$ and $m_2$ and with specified initial positions and velocities $\mathbf{r}_1$, $\mathbf{r}_2$ and $\dot{\mathbf{r}}_1$, $\dot{\mathbf{r}}_2$, we wish to solve for both bodies' subsequent motion in time, assuming gravity is the only force present in the system. Newtonian mechanics[2] provides such a complete solution, which is quite impressive, considering the simplicity of the four axioms which lead to it:

- **Newton's First Law**: An object's velocity changes only when the object is acted on by a nonzero net force.
- **Newton's Second Law**: The quantity of this force is given by $\mathbf{F} = m\mathbf{a}$, where $m$ is the mass of the object and $\mathbf{a}$ is its acceleration.
- **Newton's Third Law**: For every such action, there is an equal and opposite reaction. That is, if the above object feels a force $\mathbf{F}$, the source of the action feels a force $-\mathbf{F}$.
- **The Law of Universal Gravitation**: Given two point masses $m$ and $M$ separated by a vector $\mathbf{r}$, the force felt by $m$ due to $M$ is

[1] Throughout this section, we use 'particle' (i.e., a point mass) and 'spherical body' interchangeably – the two, if both have mass $m$, have equal gravitational effect at a radius larger than that of the spherical body, assuming the sphere is rigid and has a spherically-symmetric mass distribution [13, page 35].

[2] Why don't we instead use General Relativity, which subsumes Newton's classical model and which is ultimately a richer and more accurate description of the macroscopic universe? Because, for our undemanding astrophysical requirements here, Newtonian mechanics is plenty precise; its simplicity makes it the obvious choice when calculating orbital mechanics at this accuracy.

$$\mathbf{F} = -\frac{GmM}{r^2}\,\hat{\mathbf{r}}.$$

On the subject of minimal starting axioms, we might worry that Newton's first law is subsumed by the second, rendering the former redundant. After all, if the second law is true, then a zero net force implies a zero acceleration; is not this statement similar to that of the first law? But in fact the first law makes a far stronger claim: that of all possible physical effects, there *exist* no others (besides that of force) which may alter a body's velocity. Thus the first law is the necessary foundation upon which the second is built.

### 2.1.1 Conic sections

We will give the result before deriving it: the two bodies follow elliptical paths around their common center of mass, in the case of a bound orbit; in the case of an unbound orbit, the bodies move parabolically or hyperbolically. These three curves compose the class of *conic sections*, so called because they arise from the various ways of intersecting a plane and a hollow cone. We review them briefly below.

A conic section can be described in polar form by

$$r(\theta) = \frac{a(1-e^2)}{1+e\cos\theta}. \tag{2.1}$$

The size and shape of the conic section are determined by $a$ and $e$, respectively. We discuss the geometric interpretation of $a$ and $e$ in the context of an ellipse, while keeping in mind that they also are sufficient parameters to describe also the hyperbola and parabola. An ellipse is shown in Figure 2.1. Graphically, $a$, here called the *semi-major axis*, represents the distance between the center of the ellipse and its far-most side; algebraically, $a$ is a scaling factor. Likewise, $e$, called the *eccentricity*, determines the shape of the conic section. When $e = 0$, the ellipse is a circle; as $e$ increases towards 1 the ellipse grows progressively stretched-out.

| | |
|---|---|
| Ellipse | $0 \leq e < 1$ |
| Parabola | $e = 1$ |
| Hyperbola | $e > 1$ |

Our assumption that the two bodies follow an elliptical path is historically justified: Johannes Kepler first determined it phenomenologically of the Solar System's planetary orbits [27].[3] This empirical observation, that the planets follow ellipses,

[3]Over several agonizing years, Kepler attempted fitting the orbit data of Mars, unsuccessfully, to 40 different kinds of curves, each curve requiring laborious calculation. He had initially skipped an elliptical fit, thinking the ellipse was too simple for nature. [27]

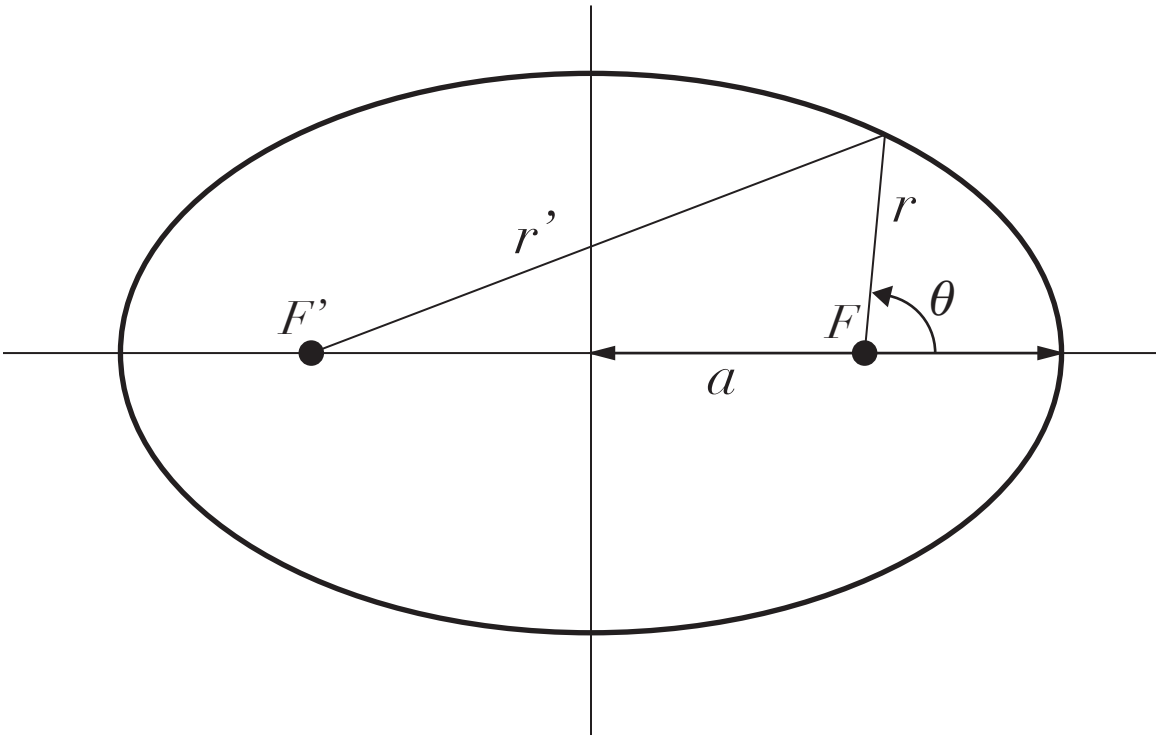


Figure 2.1: An illustration of the semi-major axis $a$, the foci $F$ and $F'$, and the polar coordinate $\theta$ for an ellipse with $e = 0.7$.

preceded a successful physical explanation (Newton's) by 80 years. And Newton, in turn, worked out his law of gravitation by starting with the assumption that bodies follow elliptical orbits [28]. Thus our following derivation of orbital motion is backwards from the original guesswork methods used by Newton and Kepler (and the many others who aren't as famous).

### 2.1.2 Choosing a coordinate system: the center-of-mass frame

We begin with a brief note on the difference between a physical system and the coordinate system (referred to colloquially as a *frame*) which measures it: A physical system consists of bodies and forces; it evolves in time and space independent of any human observation. In order to observe and measure the system's evolution – or even describe it qualitatively – the sentient observer imposes a coordinate system: this is any arrangement of quantitative measuring devices, be they yardsticks, clocks, thermometers, etc. For a given physical system, the human may concoct an infinite variety of such coordinate systems to describe it – however, only a few fit the situation naturally; the rest are useless or redundant.

Our problem of two-body orbital motion is elegantly studied and described in the center-of-mass frame. Since this is not an obvious fact, we first describe the two-body problem with a *general*, non-accelerating coordinate system and show that a center-of-mass frame greatly simplifies the physical description. Figure 2.2 depicts such an arbitrary, non-accelerating Cartesian reference frame, describing two particles of mass $m_1$ and $m_2$, with coordinates $\mathbf{r}'_1$ and $\mathbf{r}'_2$, respectively (the primes indicate the frame's generality). We will show that there exists for this physical system a unique center-of-mass frame, independent of our choice of arbitrary coordinate system; the usefulness of such a frame is that it will describe the same scenario but in fewer parameters. We start by defining the relative coordinate, $\mathbf{r}$, as

$$\mathbf{r} \equiv \mathbf{r}'_2 - \mathbf{r}'_1, \tag{2.2}$$

and the center-of-mass coordinate, $\mathbf{R}$ to be

$$\mathbf{R} \equiv \frac{m_1\mathbf{r}'_1 + m_2\mathbf{r}'_2}{m_1 + m_2}. \tag{2.3}$$

Notice that $\mathbf{r}$ is the same no matter the origin of the coordinate system, and that $\mathbf{R}$ always lies on $\mathbf{r}$ (hence the lack of primes). Rewriting the last equation for $\mathbf{R}$, we have

$$(m_1 + m_2)\mathbf{R} = m_1\mathbf{r}'_1 + m_2\mathbf{r}'_2. \tag{2.4}$$

Then, defining $M \equiv m_1 + m_2$ to be the total mass of the system, we have that

$$M\mathbf{R} = m_1\mathbf{r}'_1 + m_2\mathbf{r}'_2. \tag{2.5}$$

Assuming that the individual masses are constant in time gives

$$M\frac{d\mathbf{R}}{dt} = m_1\frac{d\mathbf{r}'_1}{dt} + m_2\frac{d\mathbf{r}'_2}{dt}, \tag{2.6}$$

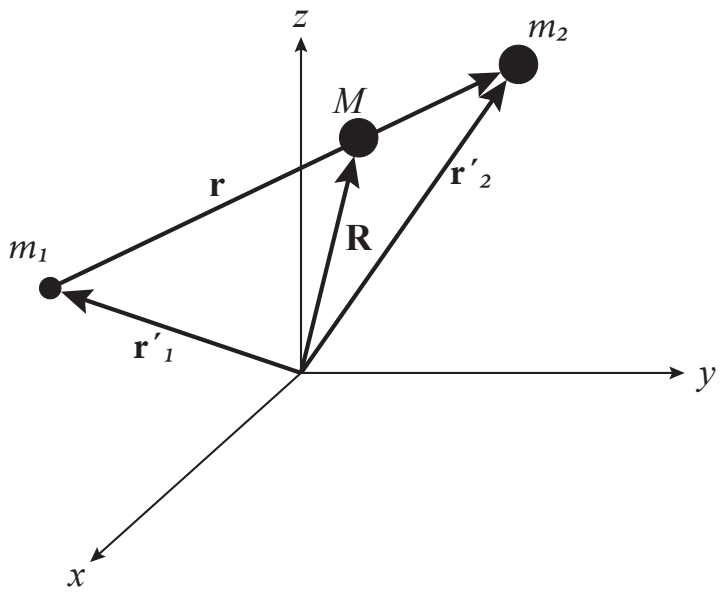


Figure 2.2: An arbitrary Cartesian coordinate system, in which $\mathbf{r} = \mathbf{r}'_2 - \mathbf{r}'_1$ is the relative coordinate, $M = m_1 + m_2$ is the total mass of the system, and $\mathbf{R} = (m_1\mathbf{r}'_1 + m_2\mathbf{r}'_2)/(m_1 + m_2)$ is the center-of-mass coordinate.

or

$$M\mathbf{V} = m_1\mathbf{v}_1' + m_2\mathbf{v}_2'. \tag{2.7}$$

Thus since $\mathbf{R}$ is the center of mass of the system, $\mathbf{V}$ is its velocity. Letting $\mathbf{P} \equiv M\mathbf{V}$ be the linear momentum of the center of mass and $\mathbf{p}_i = m_i\mathbf{v}_i$ be the linear momentum of an individual particle $i$, differentiating Equation 2.7 with respect to time yields

$$\frac{d\mathbf{P}}{dt} = \frac{d\mathbf{p}_1}{dt} + \frac{d\mathbf{p}_2}{dt}. \tag{2.8}$$

We assume that all forces on the two bodies are due strictly to each other – that is, all forces are internal to the system. Then by Newton's third law (whose general form says that the net sum of internal forces must exactly cancel out), the net force on the system is

$$F = \frac{d\mathbf{P}}{dt} = M\frac{d^2\mathbf{R}}{dt^2} = 0. \tag{2.9}$$

Then we have, by Newton's second law, that the center of mass $\mathbf{R}$ will not accelerate if there are no external forces. Thus we choose the "center-of-mass frame" as that for which $\mathbf{R} = \mathbf{V} = 0$, or, spatially speaking, the frame whose origin is locked onto the physical system's center of mass.

Thus, given that our two masses are located at points $\mathbf{r}_1'$ and $\mathbf{r}_2'$, defined in an arbitrary reference frame (as was shown in Figure 2.2), there exists a center-of-mass frame unique to the system. We can transform to such a frame via

$$\begin{aligned} \mathbf{r}_1 &= \mathbf{r}_1' - \mathbf{R} \\ \mathbf{r}_2 &= \mathbf{r}_2' - \mathbf{R}. \end{aligned} \tag{2.10}$$

(The primes are dropped to indicate a center-of-mass frame). By plugging in for $\mathbf{R}$ as defined in Eq. 2.3 and performing some algebra, we can write

$$\mathbf{r}_1 = -\frac{m_2}{m_1 + m_2}\mathbf{r} \tag{2.11}$$

$$\mathbf{r}_2 = \frac{m_1}{m_1 + m_2}\mathbf{r}. \tag{2.12}$$

Here, we define a convenient quantity, the *reduced mass*, to be

$$\mu = \frac{m_1 m_2}{m_1 + m_2}; \tag{2.13}$$

then $\mathbf{r}_1$ and $\mathbf{r}_2$ become

$$\mathbf{r}_1 = -\frac{\mu}{m_1}\mathbf{r} \tag{2.14}$$

$$\mathbf{r}_2 = \frac{\mu}{m_2}\mathbf{r}. \tag{2.15}$$

This is elegant indeed: in the center-of-mass frame, both bodies' locations are described by the same relative coordinate $\mathbf{r}$, each multiplied by a distinguishing constant. We see that then the total energy and angular momentum are simplified too: whereas for a general frame, they'd be written

$$E = \frac{1}{2}(m_1 v_1'^2 + m_2 v_2'^2) - G\frac{m_1 m_2}{|\mathbf{r}_2' - \mathbf{r}_1'|}$$

and

$$\mathbf{L} = m_1(\mathbf{r}_1 \times \mathbf{v}_1) + m_2(\mathbf{r}_2 \times \mathbf{v}_2),$$

in relative coordinates, using Equations 2.2 and 2.43, a bit of algebraic manipulation yields the simpler forms

$$E = \frac{1}{2}\mu v^2 - G\frac{(m_1 + m_2)\mu}{r} \tag{2.16}$$

and

$$\mathbf{L} = \mu \mathbf{r} \times \mathbf{v} = \mathbf{r} \times \mathbf{p}, \tag{2.17}$$

where $\mathbf{p} = \mu\mathbf{v}$. Now we see the algebraic benefit of the center-of-mass frame.

### 2.1.3 The Reduced Mass system

For a final refinement of coordinate description, we introduce a dynamically equivalent physical system to that above, the *reduced-mass system*, which is yet simpler to study. It is a hypothetical two-body construct (see Figure 2.3) with equivalent parameters $\mathbf{r}$, $\dot{\mathbf{r}}$, $E$, and $\mathbf{L}$ to those above: consider a body of mass $M = (m_1 + m_2)$ which is locked in place at the origin of an inertial coordinate system; this body is orbited by another body of mass $\mu$ and with location and velocity ($\mathbf{r}$, $\dot{\mathbf{r}}$) and whose motion is determined by Newton's laws.[4] Notice that since the central body $M$ has zero velocity (by coordinate choice), it contributes no kinetic energy or angular momentum to the system. In this way the reduced-mass system has turned the two-body problem into a one-body problem. All following calculations will act to calculate the motion of the reduced mass.

### 2.1.4 Deriving the orbital path of the reduced mass

We perform the following calculation in polar coordinates, wherein the position vector $\mathbf{r}$ is given simply by

$$\mathbf{r} = r\hat{\mathbf{r}}(\theta). \tag{2.18}$$

[4] A clarification on something I've found confusing as a student: the "reduced mass system" would not actually be an inertial one in real life: a stationary observer would see its origin (defined to be at the mass $M$) wobbling around. The system is, instead, strictly a clever revisualization for the purpose of calculating $\mathbf{r}(t, \theta)$ and $\dot{\mathbf{r}}(t, \theta)$.

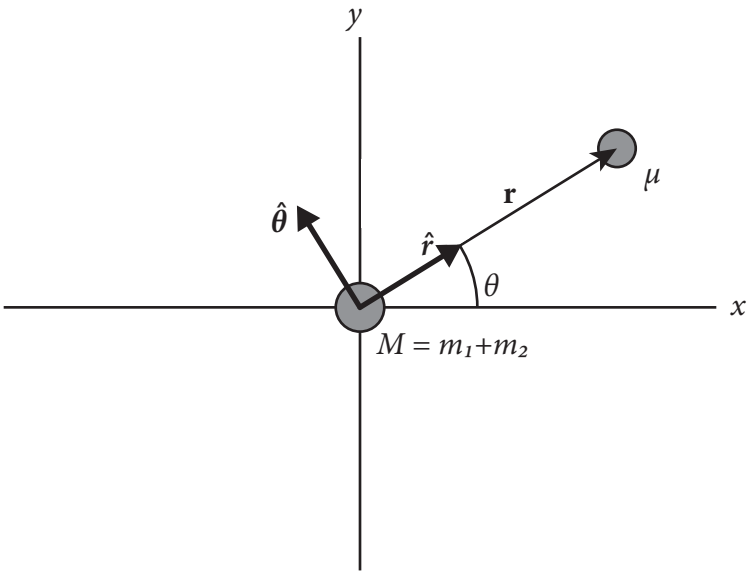


Figure 2.3: The reduced-mass system in polar coordinates.

Polar coordinates are a good choice for describing the reduced mass system because the gravitational force is, as we will see, always parallel to one of the two unit vectors, $\hat{\mathbf{r}}$, and orthogonal to the other, $\hat{\boldsymbol{\theta}}$.

Because Newton's second law ($\mathbf{F} = m\ddot{\mathbf{r}}$)[5] contains a second time-derivative, we begin by deriving an expression for acceleration $\ddot{\mathbf{r}}$ in terms of polar coordinates. Preemptively, we find the derivatives of the unit vectors $\hat{\mathbf{r}}$ and $\hat{\boldsymbol{\theta}}$ (both of which are illustrated in Fig. 2.3): Since the coordinates $r$ and $\theta$ can be expressed in terms of the cartesian $x$ and $y$ as

$$\begin{aligned} x &= r\cos\theta \\ y &= r\sin\theta, \end{aligned} \tag{2.19}$$

and likewise for the unit vectors

$$\begin{aligned} \hat{\mathbf{r}} &= \hat{\mathbf{x}}\cos\theta + \hat{\mathbf{y}}\sin\theta \\ \hat{\boldsymbol{\theta}} &= -\hat{\mathbf{x}}\sin\theta + \hat{\mathbf{y}}\cos\theta, \end{aligned} \tag{2.20}$$

we see that

$$\frac{d\hat{\mathbf{r}}}{d\theta} = \hat{\boldsymbol{\theta}}, \quad \frac{d\hat{\boldsymbol{\theta}}}{d\theta} = -\hat{\mathbf{r}}. \tag{2.21}$$

This result makes geometric sense in that $\hat{\mathbf{r}}$ and $\hat{\boldsymbol{\theta}}$ are of fixed length; any infinitesimal change to a vector which preserves its length must necessarily be in the direction perpendicular to it.

With this basic result, we can derive the time derivatives of $\mathbf{r} = r\hat{\mathbf{r}}$. Starting with the first time-derivative, we have

$$\begin{aligned} \dot{\mathbf{r}} = \frac{d\mathbf{r}}{dt} &= \frac{d}{dt}(r\hat{\mathbf{r}}) \\ &= \dot{r}\hat{\mathbf{r}} + r\frac{d\hat{\mathbf{r}}}{d\theta}\frac{d\theta}{dt} \\ &= \dot{r}\hat{\mathbf{r}} + r\dot{\theta}\hat{\boldsymbol{\theta}}. \end{aligned} \tag{2.22}$$

Taking the time derivative again gives

$$\begin{aligned} \ddot{\mathbf{r}} = \frac{d\dot{\mathbf{r}}}{dt} &= \frac{d}{dt}(\dot{r}\hat{\mathbf{r}} + r\dot{\theta}\hat{\theta}) \\ &= \ddot{\mathbf{r}}\hat{\mathbf{r}} + \dot{r}\frac{d\hat{\mathbf{r}}}{d\theta}\frac{d\theta}{dt} + \dot{r}\dot{\theta}\hat{\boldsymbol{\theta}} + r\ddot{\theta}\hat{\theta} + r\dot{\theta}\frac{d\hat{\boldsymbol{\theta}}}{d\theta}\frac{d\theta}{dt} \\ &= (\ddot{r} - r\dot{\theta}^2)\hat{\mathbf{r}} + (r\ddot{\theta} + 2\dot{r}\dot{\theta})\hat{\boldsymbol{\theta}}. \end{aligned} \tag{2.23}$$

These expressions for $\dot{\mathbf{r}}$ and $\ddot{\mathbf{r}}$ immediately imply conserved physical quantities, by a combination of the facts (1) in polar coordinates, a vector is expressed as a linear combination of $\hat{\mathbf{r}}$ and $\hat{\boldsymbol{\theta}}$; and (2) the only physical force in this system, gravity, is parallel to the former and orthogonal to the latter. Since the gravitational force acts

[5]The notation $\dot{x}$, pronounced "x-dot," denotes the first time derivative of x; two dots, $\ddot{x}$, denotes the second.

only in the $\hat{\mathbf{r}}$ direction, our task in determining the motion $\mathbf{r}(t)$ of the mass $\mu$ is to solve the two differential equations

$$\mathbf{F}_{\hat{\mathbf{r}}} = \mu(\ddot{r} - r\dot{\theta}^2) = \mathbf{F}_{gravity} \tag{2.24}$$

$$\mathbf{F}_{\hat{\theta}} = \mu(r\ddot{\theta} + 2\dot{r}\dot{\theta}) = 0. \tag{2.25}$$

These differential equations are restatements of Newton's second law. From them we determine the conserved quantities of angular momentum $\mathbf{L}$ and total energy $E$ (conserved quantities are of use to us algebraically because we will plug them in further down). First for $\mathbf{L}$: Eq. 2.25, which describes a zero angular force, encodes a conservation of angular momentum. For if we multiply both sides by $r$, we have

$$\begin{aligned} r\mu(r\ddot{\theta} + 2\dot{r}\dot{\theta}) &= \mu r^2\ddot{\theta} + 2\mu r\dot{r}\dot{\theta} \\ &= \frac{d}{dt}(\mu r^2\dot{\theta}) \\ &= \frac{d}{dt}\mathbf{L} = 0. \end{aligned} \tag{2.26}$$

Thus

$$\mu r^2\dot{\theta} = L = \text{a constant}. \tag{2.27}$$

Such a fixed angular momentum vector informs us that all motion remains in a plane, which is generally called the "plane of orbit."

The other conserved quantity that follows from Eqs. 2.24 and 2.25 is total energy $E$, because they dictate that the only force present is gravity. And gravity is a conservative force, meaning that a change in potential energy is independent of particle path. We first write $E$ in terms of polar coordinates:

$$\begin{aligned} E &= E_{\text{kinetic}} + E_{\text{potential}} \\ &= \frac{1}{2}\mu v^2 + \frac{K}{r} \\ &= \frac{1}{2}mu(\dot{r}^2 + r^2\dot{\theta}^2) + \frac{K}{r} \end{aligned} \tag{2.28}$$

where $K \equiv -GM\mu = -Gm_1m_2$. Substituting the relationship for $\dot{\theta}$ from Eq. 2.27, we remove the dependence on $\theta$:

$$E = \frac{1}{2}\mu\dot{r}^2 + \frac{L^2}{2\mu r^2} + \frac{K}{r}. \tag{2.29}$$

This is now an ordinary differential equation, whose only unknowns are $r$ and $\dot{r}$; it is tempting to solve for $\dot{r}$:

$$\dot{r} = \sqrt{\frac{2}{\mu}\left(E - \frac{K}{r} - \frac{L^2}{2\mu r^2}\right)}, \tag{2.30}$$

from which we could determine $r(t)$ by integrating both sides. However, doing so is rather laborious, and yields no closed-form solution [29]. A cleaner way to derive orbital motion, at least for our purposes, is to instead determine the path $r(\theta)$. We again remove the $\dot{\theta}$ dependence, this time substituting from Eq. 2.27 into Eq. 2.24, giving

$$\mu\ddot{r} - \frac{L^2}{\mu r^3} = F_{gravity} = \frac{K}{r^2},$$

or, upon rearrangement,

$$\mu\ddot{r} = \frac{K}{r^2} + \frac{L^2}{\mu r^3}. \tag{2.31}$$

As a reminder of how little descended this differential equation is from our starting point, its building blocks, Eqs. 2.27 and 2.24, are both derived directly from Newton's second law and the law of gravity, expressed in polar coordinates.

As a finishing move, we wish convert Eq. 2.31 into an ordinary differential equation with only $\theta$ derivatives, by means of again using the conservation of angular momentum (Eq. 2.27). But before we do, it turns out that the algebra is cleaner if we make the substitution

$$u = \frac{1}{r}. \tag{2.32}$$

Our new goal is to determine $u(\theta)$. Using Eqs. 2.32 and 2.27, we obtain new expressions for $\dot{r}$ and $\ddot{r}$:

$$\begin{aligned}
\dot{r} &= \frac{d}{dt}(\frac{1}{u}) \\
&= -\frac{1}{u^2}\dot{u} \\
&= -\frac{1}{u^2}\frac{du}{d\theta}\dot{\theta} = -r^2\dot{\theta}\frac{du}{d\theta} \\
&= -\frac{L}{\mu}\frac{du}{d\theta},
\end{aligned} \tag{2.33}$$

and

$$\ddot{r} = -\frac{L}{\mu}\frac{d^2u}{d\theta^2}\dot{\theta} = \frac{L^2u^2}{\mu^2}\frac{d^2u}{d\theta^2}. \tag{2.34}$$

Substituting these new expressions for $\dot{r}$ and $\ddot{r}$ into Eq. 2.31 and multiplying both sides by $-\mu/(L^2u^2)$ to clean up the result, we arrive at the differential equation for the path of the orbit in terms of $u(\theta)$:

$$\frac{d^2u}{d\theta^2} + u = -\frac{\mu K}{L^2}. \tag{2.35}$$

This equation has the same form as that of a harmonic oscillator subject to a constant force. The general solution for Eq. 2.35 is

$$u = -\frac{\mu K}{L^2} + A\cos(\theta - \theta_0), \tag{2.36}$$

or, in terms of $r = 1/u$,

$$r = \frac{1}{-\frac{\mu K}{L^2} + A\cos(\theta - \theta_0)}, \tag{2.37}$$

where $A$ and $\theta_0$ are arbitrary constants. Eq. 2.37 has the algebraic form of a conic section with focus at $r = 0$. Our choice of $\theta_0$ determines the orientation of the orbit in the plane, so we set $\theta_0 = 0$.

We can determine the constant $A$ by considering the turning points of the orbit – those maximum and minimum radii achieved throughout the period. Eq. 2.37 says that such extrema occur when the cosine is 1 and $-1$; that is, when $\theta = 0$ and $\theta = \pi$:

$$\begin{aligned} \frac{1}{r_{\max}} &= -\frac{\mu K}{L^2} + A \\ \frac{1}{r_{\min}} &= -\frac{\mu K}{L^2} - A, \end{aligned} \tag{2.38}$$

assuming $A$ is positive. The remaining piece of information which lets us solve for $A$ is that at such extrema, $\dot{r}$ is necessarily 0. To that end, we invoke the expression for the system's total energy, Eq. 2.29, which simplifies into the quadratic equation

$$E = 0 + \frac{L^2}{2\mu r^2} + \frac{K}{r}. \tag{2.39}$$

Solving Eq. 2.39 for $1/r$ gives

$$\begin{aligned} \frac{1}{r} &= \frac{-\mu K \pm \sqrt{2EL^2\mu + K^2\mu^2}}{L^2} \\ &= -\frac{\mu K}{L^2} \pm \frac{\sqrt{2EL^2\mu + K^2\mu^2}}{L^2} \end{aligned} \tag{2.40}$$

Noticing that Eq. 2.40 has the same form as Eq. 2.38, we identify $A$ as

$$A = \frac{\sqrt{2EL^2\mu + K^2\mu^2}}{L^2}. \tag{2.41}$$

The orbital path of the reduced mass is now solved in terms of our initial parameters; we've attained the stated goal of this section. But we'd like to adjust the resulting expression (Eq. 2.41 plugged into Eq. 2.37) to look like that of the conic section we're used to seeing,

$$r = \frac{a(1 - e^2)}{1 + e\cos\theta}. \tag{2.42}$$

Such an algebraic adjustment turns out to be a lengthy process in itself, but it is ultimately worth it. The rearrangement is useful not only for the sake of seeing the derivation from start to finish, but also for considerably simplifying the result.

We first derive the relation between semi-major axis $a$ and total energy $E$ by exploiting the extrema of the conic section given by Eq. 2.42. These turning points grant us yet more utility, in that not only do they feature $\dot{r} = 0$, but also their velocity $\mathbf{v}$ and position $\mathbf{r}$ are perpendicular; this reduces the angular momentum's vector cross-product to a multiplication of scalars. To this end, we first note that the minimum and maximum radii (here renamed, for brevity's sake, $r_p$ [periapsis] and $r_a$ [apoasis], respectively) are given by Eq. 2.42 as

$$\begin{aligned} r_p \equiv r_{min} = r(0) &= \frac{a(1-e^2)}{1+e} = a(1-e) \\ r_a \equiv r_{max} = r(\pi) &= \frac{a(1-e^2)}{1-e} = a(1+e). \end{aligned} \tag{2.43}$$

Next, since $\mathbf{L} = \mu\,\mathbf{r} \times \mathbf{v}$ is a conserved quantity (we choose to write $\mathbf{v}$ here instead of $\dot{\mathbf{r}}$ to avoid confusion between the vector and the coordinate), and because the velocities and position vectors are perpendicular at the extrema, we have that

$$\begin{aligned} \mu(\mathbf{r}_p \times \mathbf{v}_p) &= \mu(\mathbf{r}_a \times \mathbf{v}_a) \\ \mu r_p v_p &= \mu r_a v_a \\ r_p v_p &= r_a v_a \\ a(1-e)v_p &= a(1+e)v_a \\ (1-e)v_p &= (1+e)v_a. \\ v_a &= \frac{1-e}{1+e} v_p \end{aligned} \tag{2.44}$$

If we combine the results of Eqs. 2.43 and 2.44 with the expression for total energy $E = (1/2)\mu v^2 + K/r$, we have

$$\begin{aligned} E_p &= E_a \\ \frac{1}{2}\mu v_p^2 + \frac{K}{r_p} &= \frac{1}{2}\mu v_a^2 + \frac{K}{r_a} \\ \frac{1}{2}\mu v_p^2 + \frac{K}{a(1-e)} &= \frac{1}{2}\mu(\frac{1-e}{1+e}v_p)^2 + \frac{K}{a(1+e)}. \end{aligned} \tag{2.45}$$

We solve the above equation for $v_p$:

$$v_p = \sqrt{-\frac{K}{\mu a}\left(\frac{1+e}{1-e}\right)}. \tag{2.46}$$

Note that the argument of the square root is actually positive, since $K \equiv -GM\mu$. We plug this value of $v_p$ into the total energy to derive the relationship desired:

$$\begin{aligned} E &= \frac{1}{2}\mu v_p^2 + \frac{K}{r_p} \\ &= \frac{1}{2}\mu\bigg[ - \frac{K}{\mu a}\bigg(\frac{1+e}{1-e}\bigg)\bigg] + \frac{K}{a(1-e)} \\ &= \frac{K}{a(1-e)}\bigg( - \frac{1+e}{2} + 1\bigg) \\ &= \frac{K}{2a} \\ &= -\frac{GM\mu}{2a}. \end{aligned} \tag{2.47}$$

This result is fundamental – that the total energy is inversely proportional to the semi-major axis. We can now obtain an expression for the eccentricity $e$, altering the denominator of Eq. 2.37's right-hand side to match the desired form of $(1 + e\cos\theta)$. Doing so amounts to multiplying the old denominator through by $-\frac{L^2}{\mu K}$, resulting in

$$\begin{aligned} e &= (-)\frac{L^2}{\mu K}\cdot A \\ &= \frac{L^2}{\mu K}\cdot\frac{\sqrt{2EL^2\mu + K^2\mu^2}}{L^2} \qquad \text{(from Eq. 2.41)} \\ &= \sqrt{\frac{2EL^2}{\mu K^2} + 1} \\ &= \sqrt{\frac{K}{2a}\cdot\frac{2L^2}{\mu K^2} + 1} \qquad \text{(from Eq. 2.47)} \\ &= \sqrt{\frac{L^2}{\mu K a} + 1} \\ &= \sqrt{1 - \frac{L^2}{\mu^2 GMa}}. \end{aligned} \tag{2.48}$$

Thus we have solved for $a$ and $e$ of the conic section of the orbit path, completing this section. For the purposes of this thesis, every two-body orbit is completely characterized by the four parameters $m_1, m_2, a$, and $e$.

As a note, notice that bound orbits, which necessarily have $0 \leq e < 1$, must also have, by Eq. 2.47, a positive semi-major axis $(0 < a)$, and then by Eq. 2.47, a negative total energy $(E < 0)$.

We are now ready to compute the change to a two-body system's orbit caused by a supernova.

## 2.2 Our Simple Model of a Supernova

The model of supernova we use is a relatively simple event (see Section 1.4.4 for a basic explanation of the physical processes involved). We assume the explosion occurs instantly, causing only the two following effects upon the star:

(1) the star receives a kick velocity $\mathbf{v}_k$;

(2) the star loses mass of $\Delta M$.

For an illustration of the before- and after-scenarios, see Fig. 2.4. The approximation that the supernova happens in zero time is justified because the ejected material leaves the system on the order of minutes, while the planet orbits the star on at least an order of hours. So from an orbital perspective, there is very little difference between whether the explosion happened over a very short time or no time at all. On another note about our assumptions, although intuition might tell us that the planet should feel a strong blow from the blast's shock wave, in this simplified model, the planet's trajectory is completely unaffected. This simplification is physically justifiable because of the planet's relatively small surface area and its extreme distance from the star – any force imparted by the outflow of material is insignificant [30].

## 2.3 Solving for the Effect of a Supernova On a Two-Body System

Now, our goal is to find the new orbital parameters, in terms of the old, caused by the supernova. That is, we seek a mapping $\rho$, where

$$\rho : (a_0, e_0, M_0, M_1, m, \mathbf{v}_k, \theta_0) \rightarrow (a_1, e_1).$$

The variables are defined in Table 2.1.

To describe the physical scenario: Initially, a planet of mass $m$ orbits a main-sequence star of mass $M_0$; the orbital system is described by semi-major axis $a_0$ and eccentricity $e_0$. Given that the supernova occurs when the planet is at the orbital phase $\phi$, we find the relative velocities and locations between the star and planet just after the explosion. This information will directly lead to the orbital characteristics of the new system, using the results of Section 2.1.

The initial relative coordinate is given by the equation for an ellipse in polar form:

$$r(\theta) = \frac{a_0(1 - e_0^2)}{1 + e_0 cos(\theta)} \tag{2.49}$$

Then let $r_\phi$ be the relative coordinate $r(\phi)$ at the moment of explosion. We see that $r_\phi$ is not altered by the explosion, as neither the star nor the planet change position during that instant (thus we don't bother with 0 or 1 subscripts for $r_\phi$).

We compute the initial relative velocity $V_0$ at the fatal moment from energy considerations. By Eq. 2.28, the system initially has energy

$$E_0 = -\frac{GM_0m}{2a_0} = -\frac{GM_0m}{r_\phi} + \frac{1}{2}\mu_0 V_0^2, \tag{2.50}$$

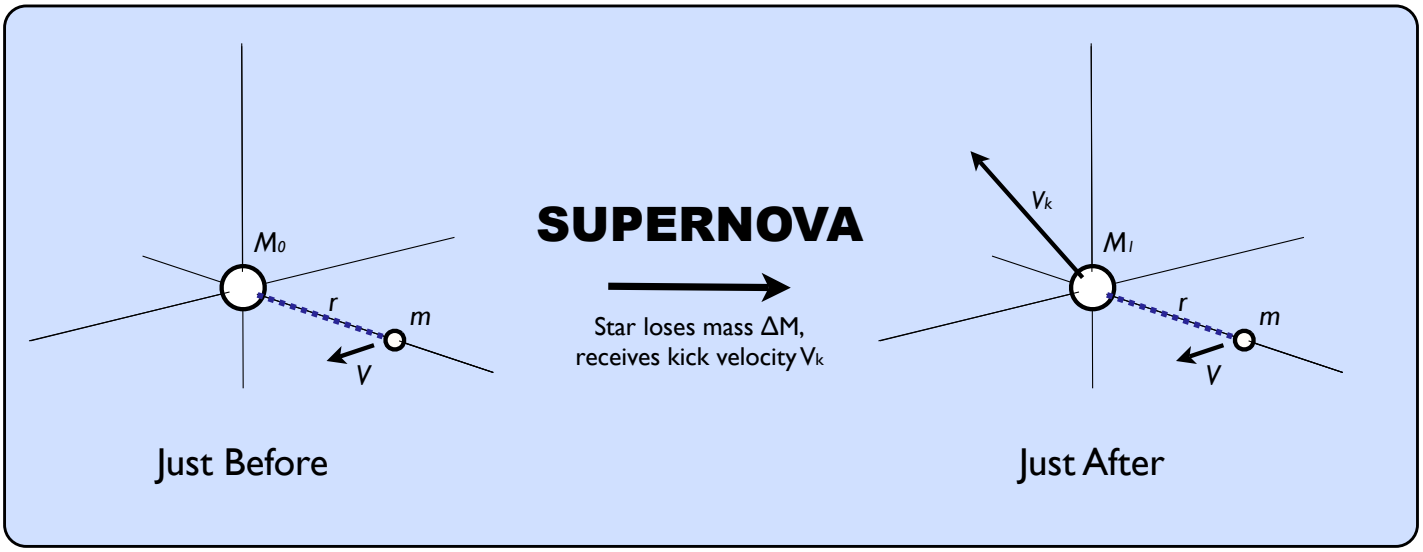


Figure 2.4: We model the supernova event as an instantaneous event: the star loses mass $\Delta M$ and receives kick velocity $\mathbf{v}_k$. Note that the planet's mass and trajectory are unaffected in our model.

where $\mu_0 = (M_0 m)/(M_0 + m)$ is the initial reduced mass of the system. Solving Eq. (2.50) for $V_0$ gives

$$V_0 = \sqrt{2G(M_0 + m)(\frac{1}{r_\phi} - \frac{1}{2a_0})} \tag{2.51}$$

Then the *new* relative velocity $\mathbf{V}_1$ is, given the addition of a kick velocity $\mathbf{v}_k$,

$$\mathbf{V}_1 = \mathbf{V}_0 + \mathbf{v}_k. \tag{2.52}$$

Plugging it into Eq. 2.28 gives the new total energy $E_1$ as

$$E_1 = -\frac{GM_1 m}{r_\phi} + \frac{1}{2}\mu_1 V_1^2. \tag{2.53}$$

Then, referencing Eq. 2.47, we obtain an expression for $a_1$:

$$\boxed{a_1 = \frac{GM_1 m}{2E_1}} \tag{2.54}$$

The new eccentricity is then, by Eq. 2.48,

$$\boxed{e_1 = \sqrt{1 - \frac{L^2}{\mu^2 MGa_1}},} \tag{2.55}$$

where $L = \mu_1(\mathbf{r}_\phi \times \mathbf{V}_1)$. Eqs. 2.54 and 2.55 are the two equations used by our simulation code. They are straightforward and don't offer a lot of physical insight, besides whether the resulting orbit is bounded ($0 \leq e_1 < 1$). However, there are other, more intuitive ways of expressing the change caused to an orbit by a supernova. An excellent algebraic analysis of the problem is covered in Hills (1983) [31], which considers the dynamically equivalent problem of a binary-star system where one star undergoes supernova. They show that, for instance, the new semi-major axis $a_1$ can be expressed in terms of the old:

$$\frac{a_1}{a_0} = \left[\frac{1 - (\Delta M/M_0)}{1 - (2a_0/r_\phi)(\Delta M/M_0) - (v_k^2 - V_0^2)/V_1}\right]. \tag{2.56}$$

From this expression, we see that if there is a zero kick-velocity ($\mathbf{v}_k = 0$), then the minimum mass loss $\Delta M$ required to dissociate the system is $\Delta M = M_0\, r_\phi/2a_0$ (that is, where $a_1/a_0$ becomes negative). Roughly speaking, since $r_\phi$ is usually of a similar size to $a_0$ for near-circular orbits, the system would tend to become unbound for $\Delta M > M_0/2$. In the case of a giant star exploding in supernova, since a safe lower bound for the star's mass at the moment before supernova is $M_0 = 4_\odot$ (Section 1.4.4), and the resulting neutron star has a fixed mass of $M_1 = 1.4_\odot$ (Section 1.5.1), the mass loss $\Delta M = M_0 - M_1$ is almost always greater than $M_0/2$. Thus our system is almost guaranteed to become unbound in the absence of a strong kick velocity, which, if aimed in the right direction, has a rescuing effect.

The kick velocity best serves to maintain a bounded orbit when it fires in the same direction as the initial relative orbital velocity $\mathbf{V}_1$. For in that case, the neutron star and planet would be traveling together, less likely to fly apart. Or, energetically speaking, the total energy is more likely to be negative, a requirement for bounded orbits.

## 2.4 Monte Carlo Simulation

Now we'd like to simulate what tends to happen to a given star-planet system. In the last section we showed that, given a set of initial orbital parameters ($M_0, m, a_0$, and $e_0$), then a supernova mass loss of $\Delta M$ and kick velocity $\mathbf{v}_k$ allowed us to easily calculate the new orbital parameters $(a_1, e_1)$ via the mapping $\rho$. But because the magnitude of $\mathbf{v}_k$ is given by a probability distribution (see Fig. 2.5) and the direction of the kick is perfectly random in $\mathbf{R}^3$, the new orbital parameters $(a_1, e_1)$ will themselves be defined by a distribution. Solving for this final distribution is analytically difficult, if not impossible. Instead we use the numerical Monte Carlo technique, wherein a computer generates pseudorandom numbers according to the kick velocity distribution and passes them through the mapping described by Eqs. 2.54 and 2.55 – each randomly generated $\mathbf{v}_k$ then yields a set of orbital parameters $(a_1, e_1)$.

Once we have multiple $(a_1, e_1)$ points, we have a distribution. We then add more such randomly generated $(a_1, e_1)$ duples to the distribution until it reaches a sufficient statistical stability in both variables. Our final result constitutes our predicted orbital distribution, from which we can then study survival rates.

### 2.4.1 Simulating the effect of a supernova on a single Planet-Star system

Four examples of star-planet systems we might pass through our simulation code are listed in Table 2.2, which are actual data of detected extrasolar planets and their stars [7]. This table is listed as an example only; we will not actually run our simulation code on detected planets, because (1) all planets detected are around small, non-pulsar progenitors and (2) even if such planets were detected, the intervening stellar evolution between detection and supernova would radically alter the orbit's parameters (see Section 1.4.5).

In performing a simulation on a single star-planet system, there remains one difficulty: the mapping $\rho$ is a function of a specific orbital phase $\phi$, so the simulation must generate the relative vector $r_\phi$ and velocity $V_0$ internally. But $r_\phi$ and $V_0$ vary throughout the period of a given orbit, due to the orbit's ellipticity. Only for a circular orbit could we simply use $r_\phi = a_0$. To make matters more difficult, in an elliptical orbit, (and the discovered exoplanets have had surprisingly high eccentricities [Section 1.3.2]), the planet travels at a higher velocity when close to the star than when far away; thus $\dot{\theta}$ is not constant, which would otherwise make the computation simpler.

We incorporate this non-constant orbital position and velocity by generating a list of $(r_\phi, V_0)$ over equal time-steps throughout the orbit. As mentioned beneath Eq. 2.30,

Table 2.1: The inputs and outputs for the calculation of the effect of a supernova on a planet-star system. The subscript $_{(0)}$ indicates variables before the supernova; the subscript $_{(1)}$ indicates variables after.

| | *Input* | | *Output* |
|---|---|---|---|
| $a_0$ | the initial semi-major axis of orbit | $a_1$ | the final semi-major axis |
| $e_0$ | the initial eccentricity of orbit | $e_1$ | the final eccentricity |
| $M_0$ | the initial mass of the star | | |
| $\Delta M$ | the mass lost by the star | | |
| $m$ | the mass of the planet (remains constant) | | |
| $\mathbf{v}_k$ | the kick velocity given to the star remnant (in the initial center-of-mass frame) | | |
| $\phi$ | the phase of the orbit at time of supernova | | |
| | *Variables only referenced within the calculation* | | |
| $\mathbf{r}_\phi$ | the relative vector at the time of explosion | | |
| $E_0$ | the initial total energy | | |
| $E_1$ | the new total energy | | |
| $\mathbf{V}_0$ | the initial relative velocity | | |
| $\mathbf{V}_1$ | the new relative velocity | | |
| $M_1$ | the mass of the star remnant: $M_1 = M_0 - \Delta M$ | | |

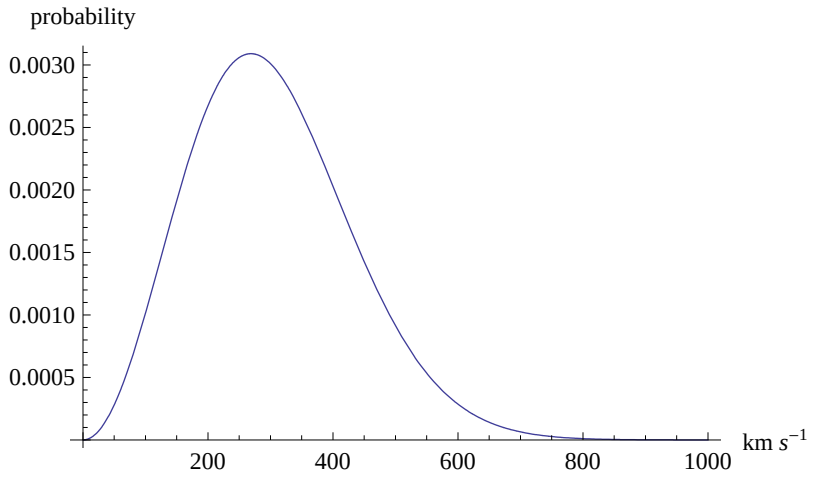


Figure 2.5: The observed distribution of pulsar velocities in the galactic frame is given by a Maxwell-Boltzmann distribution with a mean of 300 km s$^{-1}$ and a standard deviation $\sigma$ = 190 km s$^{-1}$. [Hansen, B. M., and Phinney, E. S. The pulsar kick velocity distribution. *Mon. Not. R. Astron. Soc. 291*, November 1997]

there does not exist a closed-form solution for $r(t)$ and $\theta(t)$. We instead numerically solve the motion problem, using a rearranged version of Eq. 2.27 (conservation of angular momentum) to determine the change in $\theta$:

$$d\theta = \frac{L}{\mu r^2} dt \tag{2.57}$$

Our fleshed-out algorithm is described in pseudo-code:

LocationsGenerator($M_0, m, a, e, dt$)

```
1  θ := 0 ▷ initialize the orbital phase to 0
2  t := 0
3  M := M_0 + m
4  μ := (M_0 m)/(M_0 + m)
5  L := sqrt(G M μ^2 a(1 − e^2)) ▷ angular momentum (using Eqs. 2.27, 2.28, and 2.47)
6  while θ < 2π:
7        do
8           r := (a(1 − e^2))/(1 + e cos θ)
9           dθ := L/(μ r^2) dt ▷ by Eq. 2.57
10          θ := θ + dθ
11          t := t + dt
12          record r, θ, t
```

(For the actual Mathematica code, see Appendix A).

With this code we can generate $r_\phi$ and $V_0$ at each time-step $t$, the collection of which we store in an array. Our supernova mapping $\rho$ then runs through this array, using each time-step's $r_\phi$ and $V_0$ in its computation. We end up running such circuits of the orbit array typically 100 times to achieve a statistically stable result. Thus each time-step is accessed roughly an equal number of times, satisfying our simulation requirements.

A minor complication in the above orbit-generating algorithm is that whereas highly-elliptical orbits have a wide range of radii and velocities, near-circular orbits have hardly any variation at all. Thus, computationally, it's extremely inefficient to treat each orbit with the same number of steps – the stretched-out orbit requires many, while the perfectly circular orbit requires 1. Our code thus decides the number of steps it will take based off the orbital eccentricity with the function

$$\text{steps} = \text{floor}\left[\frac{1}{0.7(1-e)}\right]. \tag{2.58}$$

We chose the coefficient 0.7 by experimenting with the code. There probably exists a better functional form for choosing the number of steps.

As an illuminating demonstration of our survival simulation code, we consider the Earth-Sun system, imagining that the Sun is hypothetically of initial mass $M_0 = 10_\odot$ and subsequently undergoes supernova. The resulting orbital distribution, plotted in Fig. 2.7, gives the Earth a 4.0% probability of remaining orbitally bound to the Sun.

| Star Name | Star Mass $M_0$ (solar masses) | Planet Mass $m$ (Jupiter masses) | $a_0$ (AU) | $e_0$ |
|---|---|---|---|---|
| HD 142 | 1.22 | 1.03 | 1.00 | .371 |
| GJ 3021 | .86 | 3.37 | .490 | .511 |
| HD 1461 | .97 | .0239 | .063 | .140 |
| HD 2039 | .99 | 4.90 | 2.2 | .67 |

Table 2.2: Four sample star-planet systems to feed to our supernova code. The code requires the four numbers $M_0, m, a_0$, and $e_0$ to define a system. As a reminder, we are not computing the survival probabilities for any such detected exoplanets; those listed here only serve as examples of the orbital description format. These data are from the NStED exoplanet database at `http://nsted.ipac.caltech.edu/index.html` [7].

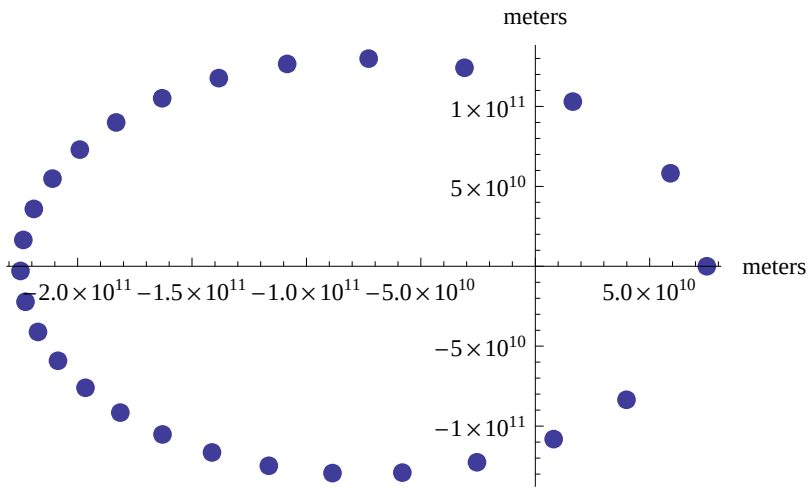


Figure 2.6: The orbital progression in constant time-steps of an Earth-mass body around a Solar-mass body in the reduced-mass frame. This orbit has an eccentricity of 0.5 and a semi-major axis of $1.5 \times 10^{11}$ meters. This figure was produced using the function `LocationsGenerator` described in Appendix A.

As we will see in the next chapter, such a survival rate is about 20 times larger than that calculated of the actual orbital systems most likely to survive.

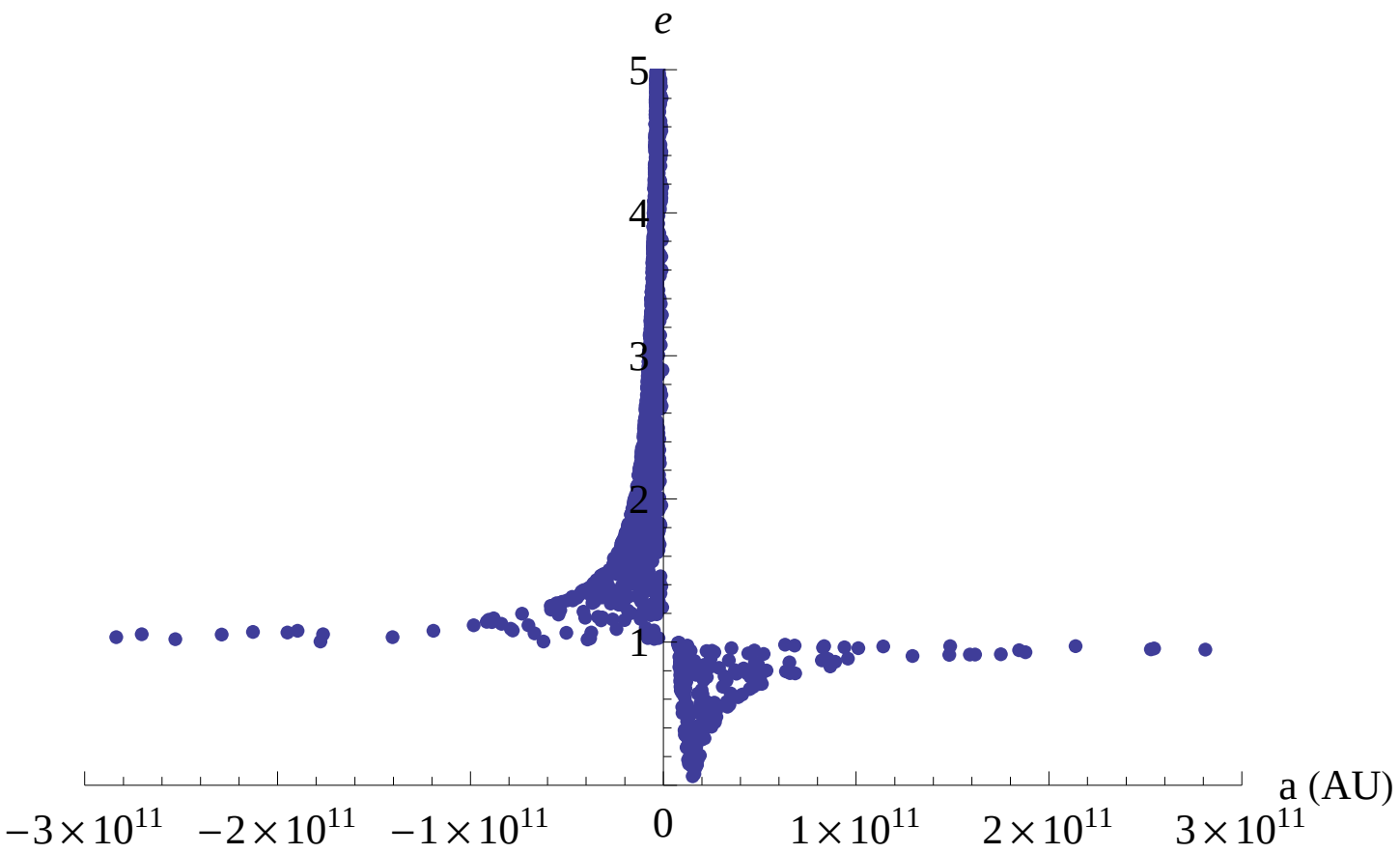


Figure 2.7: The resulting orbital distribution of the Earth-Sun system, imagining the Sun has initial mass $M_0 = 10_\odot$ and undergoes supernova. According to this simulation, the system has a 4.0% chance of remaining bound (it is unclear from the plot because the points are so large, but the distribution is actually much more dense in the unbound region). The region of bound orbits are all those for which $0 \leq e < 1$ and, equivalently, $0 < a$. This simulation is for demonstration purposes only.

# Chapter 3

# Results of the Monte Carlo Simulation

In order to study how planets are distributed around pulsar progenitors at the moment before supernova, we run our probability-of-survival simulation over a lattice of possible orbits. Those planetary orbits which result in a higher survival probability, we reason, are therefore less likely to exist in real life around pulsar progenitors, due to the observed lack of such survivors around pulsars. Those planets which we predict very unlikely to survive, on the other hand, we can say nothing about, for they contribute nothing to the pulsar planet population, even if they exist around gas giants in the first place.

To this end, the survival code was run over a range of parameters $M_0, m, a_0$, and $e_0$; the parameters were incremented in sufficiently small step sizes that the resulting distribution grew to relatively stability. Through experimentation, variation in the mass $M_0$ was found to have little effect on the survival rates, so we held it fixed at $10_\odot$. The eccentricity $e_0$ was varied from 0 through .99, as all periodic orbits were reasonable candidates, particularly given the surprisingly high eccentricities of discovered exoplanets. The semi-major axis $a_0$ was varied from 1 AU (all planets within this radius must be ruled out because of engulfment by the gas giant) through 5 AU, at which the survival probability was seen to drop off.

The resulting survival probability distribution is displayed in Fig. 3.1. It is a considerable success that the survival probabilities reach $\sim .002$, which is not a small result, considering the galactic number of pulsars is possibly on the order of $10^5$. That the simulation shows that planets with smaller semi-major axes are more likely to remain in orbit isn't terribly surprising. However, the wide fluctuation across the variation in eccentricity is unexpected, if not confusing. We expect that this fluctuation is likely due to a flaw in the simulation code, and that realistically the distribution should be smoother in $e_0$.

We can derive an upper bound for the number of planets expected to survive supernova and orbit neutron stars by assuming that all planets have the orbital parameters which maximize the likelihood of survival. In this case, the probability that no surviving planet would have been seen around a pulsar would be given by

$$p = (1 - p_s)^n \tag{3.1}$$

where $p_s$ is the survival probability and $n$ is the number of detected pulsars. Using the values $p_s = .002$ and $n = 1900$ pulsars, the resulting probability of never witnessing any surviving planet around one of the pulsars is $p = .022$. Thus, we can say that such planetary orbits, specifically those with $a_0 < 2$ AU probably don't exist around stars at that moment before supernova, because otherwise, we'd have seen them around pulsars. But, again, this assertion is weakened by its nature as an upper bound in uncertainty, and by the relatively low number of known pulsars. Were the number of detected pulsars to increase by, say, an order of magnitude and with still no survived planets, we could begin to grow confident about the implications for non-existence of certain planetary regimes.

While such a statement about planets around pulsar progenitors might be of little use at the present, it could be relevant to a future study which looks to model the planetary orbital evolution starting from planets around main-sequence stars. For if such a study concluded that planet populations were considerably dense in the orbital regime we found most likely to survive, such results would be in disagreement with our predictions. And such a disagreement would imply that at least one of the two conclusions, theirs or ours, was flawed – an instructive scientific result.

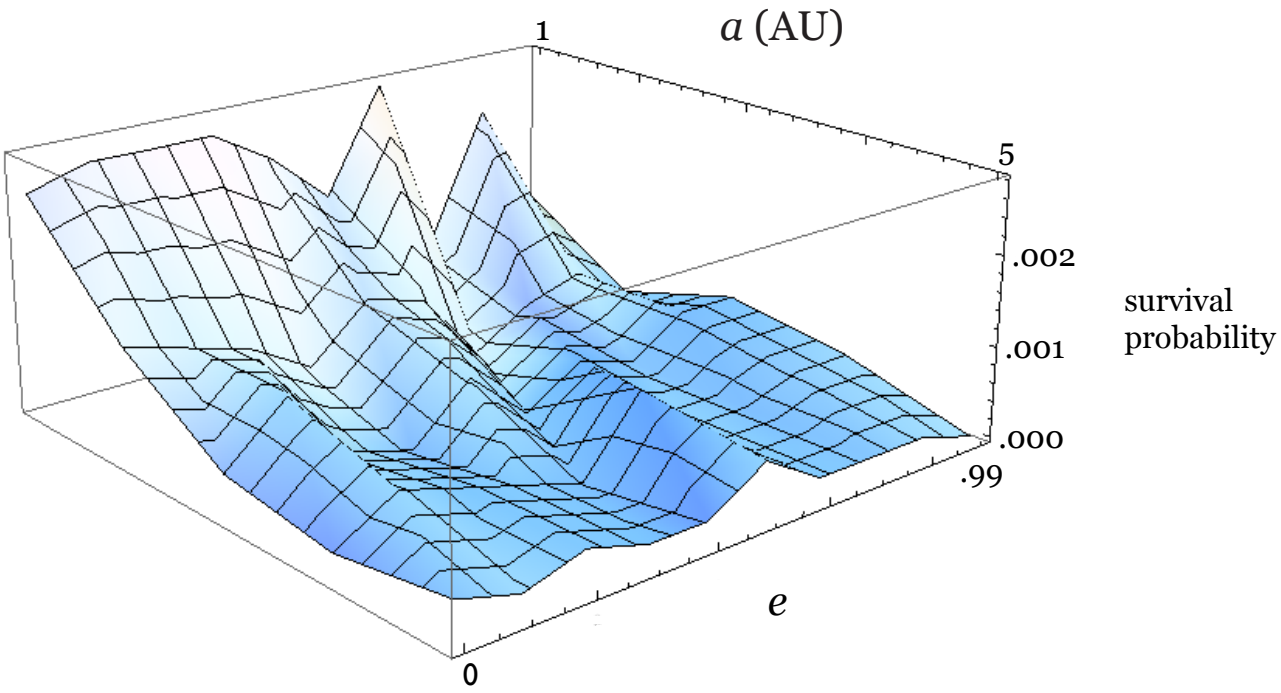


Figure 3.1: The probability distribution as calculated by our simulation. For this particular simulation, $M_0 = 10_\odot$ and $m = 2$ Jupiter masses.

# Conclusion

In this thesis, we found that the probability of planetary supernova survival is low, but not unreasonably so. We can place an upper bound on the probability of planets orbiting pulsar progenitors by assuming that all planets orbiting at the moment of supernova have the parameters of those with the maximum survival probability, $\sim$ .002. At this probability, the number of detected pulsars needs to increase by an order of magnitude before we can begin to make strong predictions about the planetary distribution around pulsar progenitors.

Further refinements could include treating with more formality the survival probabilities discussed in Chapter 3; formalizing the notion of statistical stability in Section 2.4; and a deeper algebraic analysis of the supernova's orbital effect on a two-body system, perhaps deriving analytically the maximum and minimum energies attainable in the final orbit.

# Appendix A

# Mathematica Code

*This was implemented in Mathematica 6.*

```
(* LocationsGenerator returns a list of lists {x, y, vx, vy}, each
giving the 2D position and velocity for a planet as it moves
around its orbital path in equal time steps. Each {x, y, vx, vy}
will later be used by SinglePlanet to account for the planet's
spending more time and at a lower velocity when farther away
 from its star.*)

LocationsGenerator[a_, e_, m_, M_] := Module[{G, mu, E, period, L, r,
      theta, dtheta, t, dt, x, y, V, dx, dy, vx, vy,
         steps, step, output, outputTest},
         G = 6.67*10^-11; (*gravitational constant*)
         mu = (m M)/(m + M);(*reduced mass*)
         E = -((G M m)/(2 a)); (*total energy*)
         period = Sqrt[(4pi^2)/(G (M + m)) a^3];
         L = Sqrt[G M a (1 - e^2)];(*angular momentum per unit mass*)
         steps =
            Floor[1/(.07 (1 - e))];(*steps is the number of orbit locations,
                           a function of e*)
         dt = period/steps;
        output = Table[{0, 0}, {i, 1, steps}];
        outputTest = Table[{0, 0, 0}, {i, 1, steps}];
                    (* create the output array *)
        step = 1;(*step is the location index*)
        t = 0;
        theta = 0;(* theta  is the angle of the location *)
        While[step <= steps,
              r = (a (1 - e^2))/(1 + e Cos[theta]);
               x = r Cos[theta];
               y = r Sin[theta];
               dx = (a e (1 - e^2) Cos[theta] Sin[theta])/(1 + e Cos[theta])^2
```

```
                    - (a (1 - e^2) Sin[theta])/(1 + e Cos[theta]);
              dy = (a (1 - e^2) Cos[theta])/(1 + e Cos[theta])
                    + (a e (1 - e^2) Sin[theta]^2)/(1 + e Cos[theta])^2;
                    (* dx and dy are derivatives of x and y with respect to theta *)

              V = Sqrt[2/mu ((G m M)/r + E)];
              vx = V/Sqrt[dx^2 + dy^2] dx;
              vy = V/Sqrt[dx^2 + dy^2] dy;
              output[[step]] = {x, y, vx, vy};
              outputTest[[step]] = {{x, y, dtheta}};
              step += 1;
              If[L/r^2 dt < 2, dtheta = L/r^2 dt,
                     dtheta = 2];      (*tries to prevent oversized leaps*)
              theta += dtheta;
              t += dt;
       ];

  Return[output];
  ]



(* Returns a list {a, e}, and is called by SinglePlanet. NewAE takes
a kick velocity and points it in a random direction in R^3.   Each
argument to newAE is a scalar. *)

NewAE[m_, x_, y_, vx_, vy_, kickVel_] :=  Module[{G, dxk, dyk,
       dzk, c, r, rdot, M, mu, energy, a, J, e},
        G = 6.67*10^-11;
        dxk = Random[] - .5;   (*subtract .5 to allow for vectors in other
                                          quadrants*)
        dyk = Random[] - .5;
        dzk = Random[] - .5;
        c = kickVel/Sqrt[dxk^2 + dyk^2 + dzk^2];
        r = {x, y, 0};
        rdot = {vx - (c*dxk), vy - (c*dyk), -c*dzk};
        M = 1.99*10^30(*1.4*1.99*10^30*); (*mass of neutron star*)
        mu = (m M)/(m + M);
        energy = - ((G m M)/Norm[r]) + 1/2 mu rdot.rdot;
        a = -((G m M)/(2 energy));
        J = mu Cross[r, rdot];
        e = Sqrt[1 - Norm[J]^2/(mu^2  (m + M) G a)];

        Return[{a, e}];
  ]
```

```
(* Performs the large-scale Monte Carlo simulation and returns a list \
of lists {a1, e1}, which
constitutes the distribution of orbits. *)

SinglePlanet[e_, a_, m_, M_, sims_] :=  Module[{G, vk, Locations,
      cycles, Output, outputIndex, location, j},
        G = 6.67*10^-11;
 (* kick velocity is in m/s *)
  (* Locations is a list of elements,
        each {x,y, vx, vy} *)

        Locations = LocationsGenerator[a, e, m, M];
        If[Length[Locations] <= sims,
               cycles = Floor[sims/Length[Locations]], cycles = 1];
        Output = Table[0, {k, 1, cycles*Length[Locations]}];
        outputIndex = 1;
        For[location = 1, location <= Length[Locations],
              For[j = 1, j <= cycles,
                    Output[[outputIndex]] =
                    NewAE[m, Locations[[location, 1]], Locations[[location, 2]],
                    Locations[[location, 3]], Locations[[location, 4]],
                    RandomReal[MaxwellDistribution[190*10^3]]];
                    j++;
                    outputIndex++;
               ];
         location++;
         ];

          Return[Output];
  ]




(* returns the fraction of planets which remain bound. SinglePlanetFraction
is actually a copy of the above SinglePlanet, only altered to return a fraction
instead of a list of the new orbit parameters. *)

SinglePlanetFraction[e_, a_, m_, M_, sims_] :=  Module[{G, vk, Locations, cycles,
  totalIndex, bounded, location, j},
        G = 6.67*10^-11;
        vk = 450*10^3;
```

```
        Locations = LocationsGenerator[a, e, m, M];
        If[Length[Locations] <= sims,
               cycles = Floor[sims/Length[Locations]], cycles = 1];
        totalIndex = 1;
        bounded = 0;
        For[location = 1, location <= Length[Locations],
               For[j = 1, j <= cycles, If[
                    NewAE[m, Locations[[location, 1]], Locations[[location, 2]],
                    Locations[[location, 3]], Locations[[location, 4]],
                    RandomReal[MaxwellDistribution[260*10^3]][[1]] > 0,
                    bounded++];
                    j++;
                    totalIndex++;
                ];
           location++;
    ];
  Return[N[bounded/totalIndex]];
  ]
```

# References


[1] C. Mordasini, W. Benz, Y. Alibert, *Astronomy & Astrophysics* **526**, 12 (2011).

[2] A. Wolszczan, D. A. Frail, *Nature* **355**, 145 (1992).

[3] E. B. Ford, K. J. Joshi, F. A. Rasio, B. Zbarsky, *Astrophysical Journal* pp. 336 – 350 (2000).

[4] S. Thorsett, J. A. Phillips, *Astrophysical Journal, Part 2 - Letters* **387**, L69 (1992).

[5] (International Astronomical Union (IAU), 2006). Available from: `http://www.iau.org/public_press/news/detail/iau0603/`.

[6] M. Mayor, D. Queloz, *Nature* **378**, 355 (1995).

[7] `http://nsted.ipac.caltech.edu/index.html` (2011). Available from: `http://nsted.ipac.caltech.edu/index.html`.

[8] P. Kalas, *et al.*, *Science* **322**, 1345 (2008).

[9] M. Petr-Gotzens, S. Daemgen, S. Correia, Protoplanetary disks of ttauri binaries in orion: prospects for planet formation (2009). ArXiv print. Available from: `http://arxiv.org/abs/0912.1720v1`.

[10] J. Debes, S. Sigurdsson, *Astrophysical Journal, 581, 1256* **581** (2002).

[11] F. Mullally, *et al.*, *Astrophysical Journal* **676**, 573 (2008).

[12] K. P. Schroder, R. C. Smith, *Mon. Not. R. Astron. Soc.* **000**, 1 (2008). Available from: `http://arxiv.org/abs/0801.4031v1`.

[13] B. W. Carroll, D. A. Ostlie, *Introduction to Astrophysics* (Pearson Education, Inc., publishing as Addison-Wesley, San Francisco, 2007).

[14] J.-L. Tassoul, M. Tassoul, *A Concise History of Solar and Stellar Astrophysics* (Princeton University Press, 2004).

[15] P. Demorest, T. Pennucci, S. Ransom, M. Roberts, J. Hessels, *Nature* **467**, 1081 (2010).

[16] S. Thorsett, B. Kiziltan, A. Kottas, The neutron star mass distribution. Available from: `http://arxiv.org/abs/1011.4291` [cited 2010].

[17] B. M. Hansen, E. S. Phinney, *Mon. Not. R. Astron. Soc.* **291**, 569 (1997).

[18] E. Villaver, M. Livio, *Astrophysical Journal* **661**, 1192 (2007).

[19] M. J. Duncan, J. J. Lissauer, *Icarus* p. 303 (1998).

[20] F. Lyne, A. G; Graham-Smith, *Pulsar Astronomy* (Cambridge University Press, 1990).

[21] A. Hewish, J. Bell, *Nature* **217**, 709 (1968).

[22] W. Baade, F. Zwicky, *Phys. Rev.* **46**, 76 (1934). Available from: `http://prola.aps.org/abstract/PR/v46/i1/p76_2`.

[23] F. Pacini, E. Salpeter, *Nature* **218**, 733 (1968).

[24] (2011) [cited ATNF Pulsar Catalogue]. Available from: `http://www.atnf.csiro.au/people/pulsar/psrcat/`.

[25] R. N. Manchester, G. B. Hobbs, A. Teoh, M. Hobbs, *Astrophysical Journal* **129** (2005).

[26] P. Podsiadlowski, *Planets Around Pulsars*, J. A. Phillips, S. E. Thorsett, S. R. Kulkarni, eds. (1993), vol. 36 of *ASP Conference Series*.

[27] A. Koyre, *The Astronomical Revolution* (Hermann, 1973).

[28] I. Newton, *Philosophiæ Naturalis Principia Mathematica (English Translation)* (Edmund Halley, 1729).

[29] K. R. Symon, *Mechanics* (Addison Wesley Publishing Company, 1971), third edn.

[30] R. J. Dewey, J. M. Cordes, *Astrophysical Journal* **321**, 780 (1987).

[31] J. G. Hills, *Astrophysical Journal* **267**, 322 (1983).

[32] E. Villaver, *arXiv.org/abs/1101.1773v1* (2011).

[33] R. N. Manchester, J. H. Taylor, *Pulsars* (W. H. Freeman and Company, 1977).

[34] J. H. Debes, S. Sigurdsson, *Astrophysical Journal, Letters, 668, L167* (2007).

[35] A. M. Mandel, S. Sigurdsson, *Astrophysical Journal, Letters, 599, L111* (2003).

[36] F. H. Shu, *The Physical Universe: An Introduction to Astronomy* (University Science Books, 1982).